

Sequence stratigraphy and depositional environments of the Shamokin (Union Springs) Member, Marcellus Formation, and associated strata in the middle Appalachian Basin

Daniel Kohl, Rudy Slingerland, Mike Arthur, Reed Bracht, and Terry Engelder

ABSTRACT

Organic-carbon-rich shales of the lower Marcellus Formation were deposited at the toe and basinward of a prograding clinothem associated with a Mahantango Formation delta complex centered near Harrisburg, Pennsylvania. Distribution of these organic-carbon-rich shales was influenced by shifts in the delta complex driven by changes in rates of accommodation creation and by a topographically high carbonate bank that formed along the Findlay-Algonquin arch during deposition of the Onondaga Formation. Specifically, we interpret the Union Springs member (Shamokin Member of the Marcellus Formation) and the Onondaga Formation as comprising a single third-order depositional sequence. The Onondaga Formation was deposited in the lowstand to transgressive systems tract, and the Union Springs member was deposited in the transgressive, highstand, and falling-stage systems tract. The regional extent of parasequences, systems tracts, and the interpreted depositional sequence suggest that base-level fluctuations were primarily caused by allogenic forcing—eustasy, climate, or regional thermal uplift or subsidence—instead of basement fault reactivation as argued by previous workers. Paleowater depths in the region of Marcellus Formation black mudrock accumulation were at least 330 ft (100 m) as estimated by differences in strata thickness between the northwestern carbonate

AUTHORS

DANIEL KOHL ~ *Department of Geosciences, Pennsylvania State University, University Park, Pennsylvania 16802; present address: Chevron North America Exploration and Production Company, 1550 Coraopolis Heights Road, Moon Township Pennsylvania 15108-1611; Daniel.Kohl@Chevron.com*

Daniel Kohl is a geologist working for Chevron North America. He received an M.S. degree in geoscience from the Pennsylvania State University and a B.S. degree in geology from Washington and Lee University. Currently, he works to explore and develop unconventional shale gas plays in the Appalachian Basin of the eastern United States.

RUDY SLINGERLAND ~ *Department of Geosciences, Pennsylvania State University, University Park, Pennsylvania 16802; sling@psu.edu*

Rudy Slingerland is a professor of geology at the Pennsylvania State University. He received a B.S. degree from Dickinson College and an M.S. degree and a Ph.D. from the Pennsylvania State University. Currently, his research focuses on earth surface processes, sedimentation, and stratigraphy.

MIKE ARTHUR ~ *Department of Geosciences, Pennsylvania State University, University Park, Pennsylvania 16802; maa6@psu.edu*

Mike A. Arthur, a geochemist and sedimentary geologist, is a Penn State professor of geosciences. He received B.S. and M.S. degrees from the University of California, Riverside, and a Ph.D. from Princeton University. Currently, his research focuses on studies of modern marine environments characterized by organic-carbon-rich sediment deposits.

REED BRACHT ~ *Department of Geosciences, Pennsylvania State University, University Park, Pennsylvania 16802; reed.bracht@gmail.com*

Reed Bracht is a geophysicist working for Hess Corporation. He received his B.S. degree from the University of Nebraska-Lincoln and his M.S. degree from the Pennsylvania State University. He has worked various unconventional plays, offshore Gulf of Mexico, and Equatorial Guinea, Africa.

Copyright ©2014. The American Association of Petroleum Geologists. All rights reserved.

Manuscript received July 16, 2012; provisional acceptance March 26, 2013; revised manuscript received June 26, 2013; final acceptance August 23, 2013.

DOI:10.1306/08231312124

TERRY ENGELDER ~ *Department of Geosciences, Pennsylvania State University, University Park, Pennsylvania 16802; engelder@geosc.psu.edu*

Terry Engelder is a professor of geosciences at the Pennsylvania State University. He received his B.S. degree from the Pennsylvania State University, his M.S. degree from Yale University, and his Ph.D. from Texas A&M University. He has previously served on the staff of the U.S. Geological Survey, Texaco, and Lamont-Doherty Earth Observatory. He has written 150 research articles, many focused on Appalachia, and a book, *Stress Regimes in the Lithosphere*.

ACKNOWLEDGEMENTS

We are grateful for funding provided to the Appalachian Basin Black Shale Research Group by Chesapeake Energy Corporation, Chevron North American Exploration and Production, Consol Energy, Encana Oil and Gas, EnergyPlus, ExxonMobil, Hess Corporation, Range Resources Corporation, Samson Resources, Shell Canada Energy, Southwestern Energy Company, Statoil, Talisman Energy, and Unconventionals LLC. We thank Alex Bryk, Genevieve Ellsworth, Nate Wysocki, Leah Toms, and Taylor Mclean for their help in preparing the data set and with field work and Gary Lash for sharing his compilation of logs from the Appalachian Basin. Elizabeth Hajek provided helpful reviews of earlier drafts. This manuscript benefited from comments by Terrilyn Olson, Daniel Ciulavu, and one anonymous reviewer.

The AAPG Editor thanks Senior Associate Editor Terrilyn Olson and the following reviewers: Daniel Ciulavu and an anonymous reviewer.

bank and basinal facies to the southeast. Geochemical analysis indicates anoxic to euxinic bottom-water conditions. These conditions were supported by a deep, stratified basin with a lack of circulation.

INTRODUCTION

The Marcellus Formation throughout Pennsylvania, New York, West Virginia, and Ohio is a proven unconventional natural-gas resource, potentially containing as many as 489 tcf of recoverable reserves (Engelder and Lash, 2008) and 84 tcf of undiscovered resources (Coleman et al., 2011). Since 2006, advances in horizontal drilling and high-volume hydrofracturing technology have revitalized the basin and resulted in more than 3000 wells producing from the formation. Initial well production rates vary greatly (less than 1 to more than 10 mmcf/day) and likely depend on a multitude of parameters, including completion style, reservoir quality, structural variation, stratigraphic placement of horizontal well bore, and lateral length. The large number of variables influencing well production rates presents a complex multivariate problem. Central to unraveling the variable production rates is an understanding of the subsurface facies variations as controlled by sequence stratigraphy and the depositional environment.

Previous stratigraphic work by Brett and ver Straeten (1994), ver Straeten (1996, 2004, 2007), and Brett et al. (2011) relied principally on outcrop observations in Pennsylvania, West Virginia, and New York. This study integrates these outcrop studies with cores, well logs, and geochemical data to construct a sequence-stratigraphic and depositional model for the Onondaga Formation through the Shamokin (Union Springs) and Purcell Members of the Marcellus Formation in the middle Appalachian Basin of Pennsylvania (Figure 1). Of the two organic-carbon-rich zones in the Marcellus, the lower Shamokin (Union Springs) Member is emphasized because it is the present stratigraphic target interval of many horizontal wells. The major objectives are (1) to define and describe the lithofacies and associated depositional processes and systems tracts of the lower part of the Marcellus and associated formations and (2) to construct a sequence-stratigraphic framework for predicting the lateral and vertical variability of the economically significant lithofacies in this interval. We seek to focus on the lower sequence in the Marcellus as an analog for the overlying sequences that contribute to the larger reservoir. This interval provides an excellent analog because of through-going ash beds that are used to guide sequence-stratigraphic

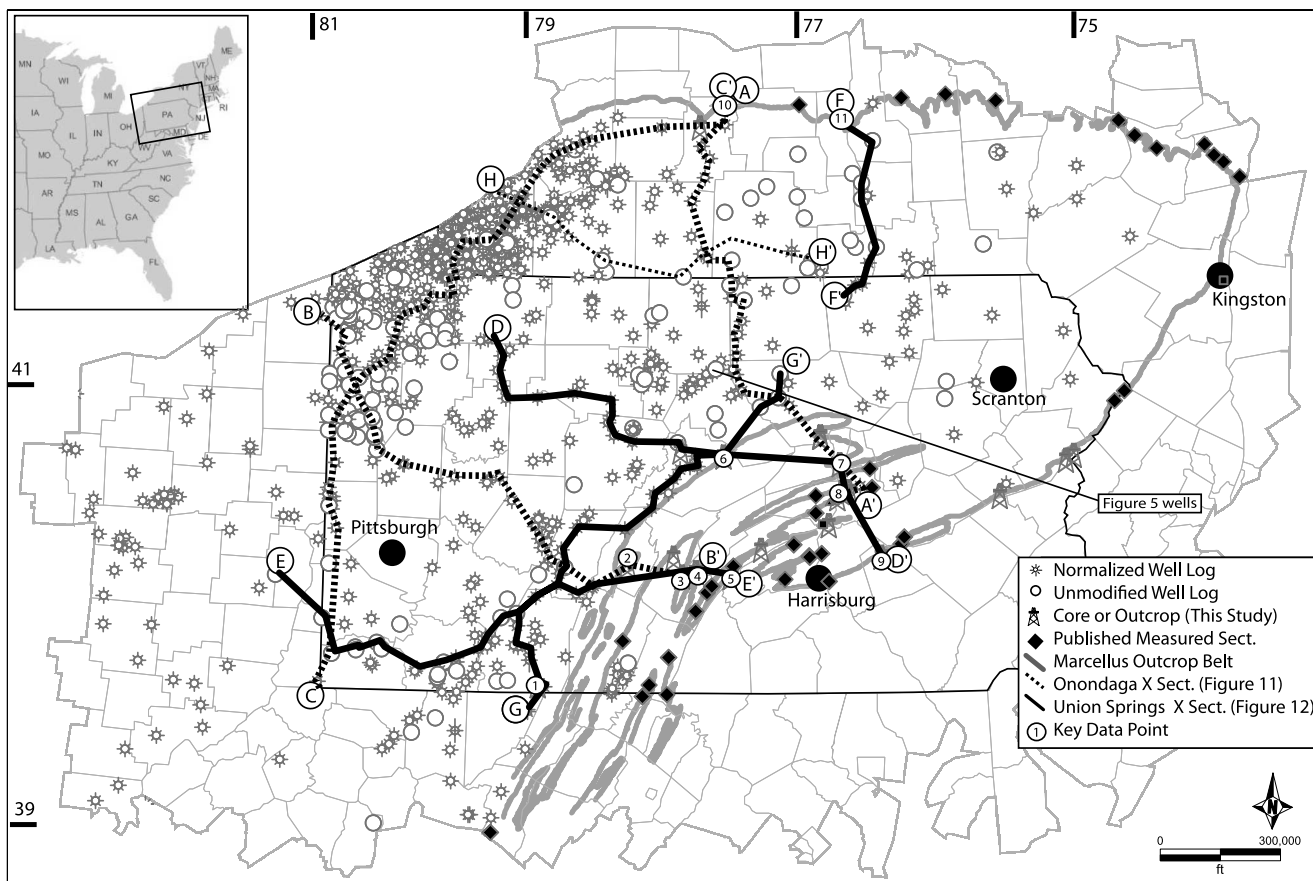


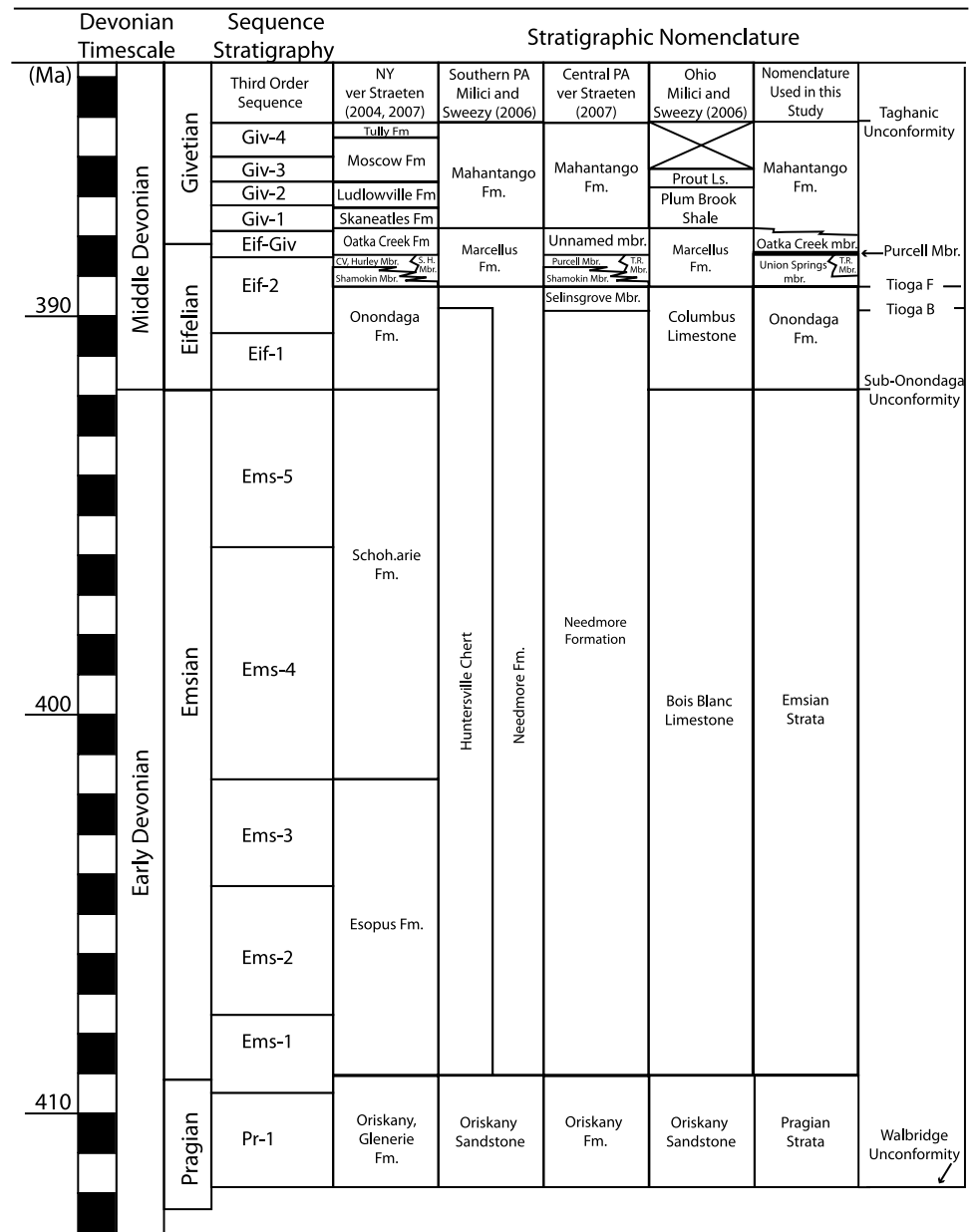
Figure 1. Map of the study area showing the Marcellus Formation outcrop belt and the locations of wells, cores, outcrops, and published measured sections used in this study. Numbers mark key localities referenced in the text: (1) Sampson 1 Yoder core, (2) Franktown outcrop, (3) Mapleton outcrop, (4) Bilger core, (5) East Waterford outcrop, (6) Bald Eagle core, (7) Erb core, (8) Handiboee core, (9) Swatara Gap outcrop, (10) Honeoye Falls outcrop, (11) Seneca Stone outcrop. Lines AA', BB', and CC' are found in Figure 11 (foldout). Lines DD', EE', FF', and GG' are found in Figure 12 (foldout). Line HH' is found in Figure 9.

interpretations and reveal synchronously deposited facies. We build on earlier subsurface work (West, 1978; Piotrowski and Harper, 1979; Rickard, 1984, 1989; de Witt et al., 1993; Lash and Engelder, 2011), but our interpretations differ in detail, systems tracts, and causes.

The Union Springs member and the underlying Onondaga Formation compose a single third-order depositional sequence. Within this sequence, we identify 10 parasequences, 3 associated with the Onondaga Formation, one transition, and six parasequences associated with the Union Springs member. We interpret the Onondaga Formation to represent the lowstand and early transgressive systems tract (TST), and the Union Springs member was deposited during the TST, highstand systems tract (HST), and falling-stage systems tract (FSST).

The overlying Purcell Member comprises the low-stand systems tract (LST) of the next depositional sequence. The upper part of the Union Springs member was deposited as part of a forced regression and is coeval with more proximal delta-front sandstones of the Mahantango Formation. As such, the thickness and spatial distribution of the reservoir facies within the Union Springs member was influenced by the progradation of this delta complex. Additionally, prior to the deposition of the Union Springs member, an as-much-as-220-ft (67-m)-thick carbonate bank with pinnacle reefs (Onondaga Formation) was deposited in the north and northwestern parts of the basin. The Union Springs member onlaps and pinches out onto this bank, which provides a minimum water depth of deposition for the organic-carbon-rich reservoir

Figure 2. Stratigraphic nomenclature of the study interval. Shown are depositional sequences of Brett et al. (2011) and ver Straeten (2007) combined with the calibrated Devonian time scale of Kaufmann (2006). This study uses the lithologic subdivision of ver Straeten (2007) for central Pennsylvania but substitutes the common member names used in the northern part of the basin (New York and northern Pennsylvania; ver Straeten, 2004). T.R. = Turkey Ridge Member; S.H. = Stony Hollow Member; CV/Hurley = Cherry Valley and Hurley Members undivided.



facies of the Union Springs member. We estimate the basin was at least 450 ft (150 m) deep during the deposition of the Union Springs.

BACKGROUND

Stratigraphy

Unit names used in this study and regional stratigraphic equivalents are given in Figure 2. We use the

term Emsian strata for all of those rocks deposited during the Emsian Age, Onondaga Formation to describe Eifelian stage limestones and calcareous shales containing the Tioga ash beds (Onondaga Formation and Selinsgrove Limestone Member of the Needmore Formation), and Marcellus Formation to describe the upper Eifelian and lower Givetian stage mudrock-dominated strata lying immediately above the Onondaga Formation. The Marcellus Formation is overlain by, and grades southeastward into, the Mahantango Formation. Although the Marcellus Formation in New York has recently been

elevated to subgroup status (ver Straeten, 2007), we retain the Pennsylvania usage subdividing it into three units. We use the informal name Union Springs member for a basal organic-carbon-rich unit (called the Shamokin Member in ver Straeten, 2007). It is succeeded by the Purcell Member, a group of limestone beds in central and western Pennsylvania, or by sandstones of the Turkey Ridge Sandstone Member to the east. The Purcell and Turkey Ridge Members are partially chronostratigraphically equivalent to the Bakoven, Cherry Valley, Hurley, and Stony Hollow units in New York (Figure 2; ver Straeten, 1996; ver Straeten and Brett, 2006). Above the Purcell and equivalents lies a second organic-carbon-rich unit that we informally call the Oatka Creek member (unnamed member in ver Straeten, 2007).

These units sit within the Pragian-1 through Givetian-4 lower Kaskaskia supersequence, which is bounded below by the Walbridge unconformity or correlative conformity and above by the Taghanic unconformity or correlative conformity (Sloss, 1963; Johnson et al., 1985) and spans approximately 28.5 m.y. (Kaufmann, 2006) (Figure 2). Various researchers have presented sequence-stratigraphic frameworks and sea level curves for the lower Kaskaskia (Dennison and Head, 1975; Johnson et al., 1985; Brett, 1998; Bartholomew and Brett, 2007; Desantis et al., 2007; ver Straeten, 2007; ver Straeten et al., 2010; Lash and Engelder, 2011). Here, we use the framework of ver Straeten (2007), who divides the lower Kaskaskia sequence into 13 third-order depositional sequences.

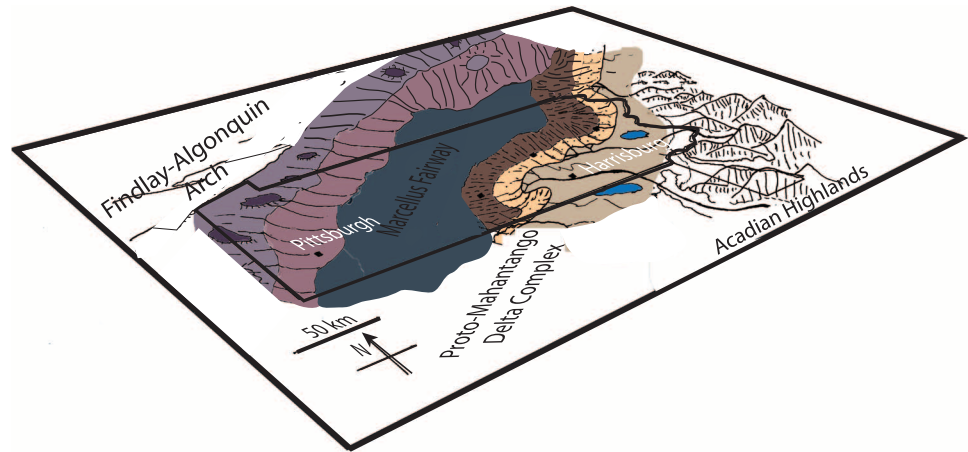
Emsian strata overlie a sharp flooding surface at the top of Pragian strata or the Walbridge unconformity (Inners, 1975; Faill et al., 1978; ver Straeten, 1996; ver Straeten and Brett, 2006) and are capped by the sub-Onondaga unconformity or correlative conformity. They generally increase in thickness from zero in northwestern Pennsylvania to more than 500 ft (152 m) at the southeastern edge of the outcrop belt. Emsian strata deposited in shallower water at the northwestern edge of the basin (e.g., Bois Blanc Limestone) grade to the southeast into more basinal facies (Huntersville Chert, Needmore Shale) and to the east into relatively shallow-water clastic-dominated facies (e.g.,

Schoharie Formation and Palmerton Sandstone) (Epstein et al., 1974; Dennison and Head, 1975; Inners, 1975; Dennison and Hasson, 1976; Epstein, 1984).

Eifelian stage strata overlie the sub-Onondaga unconformity or correlative conformity (Inners, 1975; ver Straeten, 1996, 2007) and are divided into three depositional sequences by Brett et al. (2011): Eif-1, Eif-2, and Eif-Giv. The base of Eif-2 is generally conformable; the base of the Eif-Giv is defined as the base of the Purcell Member or a horizon within the Turkey Ridge Sandstone Member (ver Straeten, 2007; Brett et al., 2011). Eif-1 and Eif-2 strata comprise the Onondaga Formation in Pennsylvania and New York, consisting of a variety of facies ranging from black calcareous mudstones to fossiliferous grainstones and biohermal reefs (Oliver, 1954, 1956; Wolosz, 1992; ver Straeten and Brett, 1995; ver Straeten and Brett, 2000). Relatively shallow-water facies in western and northeastern Pennsylvania and New York thin and fine southeastward, grading into deeper water facies characterized by thin- to medium-bedded argillaceous wackestones and micrite limestones interbedded with calcareous shales (Inners, 1975; ver Straeten, 1996, 2007). Eif-Giv strata consist of carbonates, sandstones, and black shales of the Purcell, Stony Hollow, and Oatka Creek units of the Marcellus Formation.

Chronostratigraphic and biostratigraphic data (summarized in Brett et al., 2011) combined with calibration of the Devonian time scale indicate that the Onondaga Formation (Eif-1, early Eif-2) was deposited between approximately 391.9 ± 3.4 and 390 ± 0.5 Ma (Kaufmann, 2006). The presence of the Kačák-otomari bioevent in the lower Oatka Creek member (Eif-Giv; Brett et al., 2011) suggests that the Union Springs member was deposited between approximately 390 ± 0.5 and 388.1 ± 2.6 Ma (Kaufmann, 2006). Thus, the maximum sedimentation rate in northeast Pennsylvania of approximately 50 ft/m.y. (15 m/m.y.) in the Pragian and Emsian stages increased to approximately 100 ft/m.y. (30.5 m/m.y.) in the Eifelian stage and reached a maximum sedimentation rate of approximately 250 ft/m.y. (76 m/m.y.) in the Givetian stage.

Figure 3. Generalized Middle Devonian Acadian foreland basin paleogeography based on data from Castle (2001), Prave et al. (1996), and data from this study. The western part of the basin was persistent paleotopographic high and carbonate depocenter. The central basin was dominated by argillaceous strata; the eastern basin contains a clastic-dominated shoreline fed by the Acadian highlands farther to the east.



Tectonic, Climatic, and Oceanic Setting

The strata examined in this study were deposited in the Middle Devonian Acadian foreland basin of eastern North America (Figure 3). This basin was elongate, trending northeast to southwest, and bounded to the southeast by the Acadian highlands and to the northwest by the Findlay-Algonquin arch (Ettensohn, 1985; Castle, 2001). The basin was created by thrust-load-induced subsidence caused by oblique collision between the Avalonian microplate and Laurentia in the Late Silurian through Late Devonian. Flexural modeling based on observed stratal thicknesses indicates approximately 1.2 mi (2 km) of crustal thickening occurred in eastern Pennsylvania, New Jersey, and southeasternmost New York (Beaumont et al., 1988). Clastic detritus from this orogenic landmass was shed northwestward into the basin (Ettensohn, 1985; Beaumont et al., 1988). Following the creation of the early Pragian Walbridge unconformity (Sloss, 1963), the basin was flooded from the southwest by marine waters of the Rheic Ocean. Basin paleobathymetry during the Middle Devonian is uncertain, but a fringe of Onondaga Formation reefs across New York state indicates a general shoaling to the northwest, north, and northeast (Mesolella, 1978; Edinger et al., 2002).

During the Middle Devonian, the distal (northwest) part of this foreland basin was not bounded by a traditional flexural forebulge, but instead was defined by the Findlay-Algonquin arch, a topographic high that resulted from the interaction of the Acadian foredeep and the intracratonic

Michigan Basin (Beaumont et al., 1988). As indicated by higher sedimentation rates in the Michigan Basin during this time (Beaumont et al., 1988), a correspondingly greater lithospheric load likely acted there. Interaction with the Acadian loads created significantly lower accommodation rates on the arch and promoted numerous unconformities. These surfaces become generally conformable to the east toward the Acadian foredeep.

In the Middle Devonian the Laurentian continent was located at 25°–35°S within the subtropical climate belt (Scotese and McKerrow, 1990; Edinger et al., 2002). This climate promoted the deposition of carbonates that combined with clastic detritus shed from the Acadian highlands to produce a mixed clastic-carbonate depositional system (Brett and Baird, 1985). Given the cul-de-sac basin geometry and subtropical setting, circulation in this epeiric sea probably was quasi-estuarine, driven by freshwater runoff from the Acadian highlands (McCollum, 1988; Ericksen et al., 1989). Whether the seaway was ever shallow and hypersaline in the Middle Devonian as suggested by McCollum (1988) will be commented on below. At relative highstands and as increased crustal loading occurred through the late Eifelian into the Givetian, the seaway became more open, as indicated by drowned reefs and a foredeep in eastern Pennsylvania and New York. Waters were warm (~25°–35°C), as indicated by tropical-type fossils in the Onondaga reefs and $\delta^{18}\text{O}$ signatures from Hamilton Group brachiopods (Milici and Swezey, 2006).

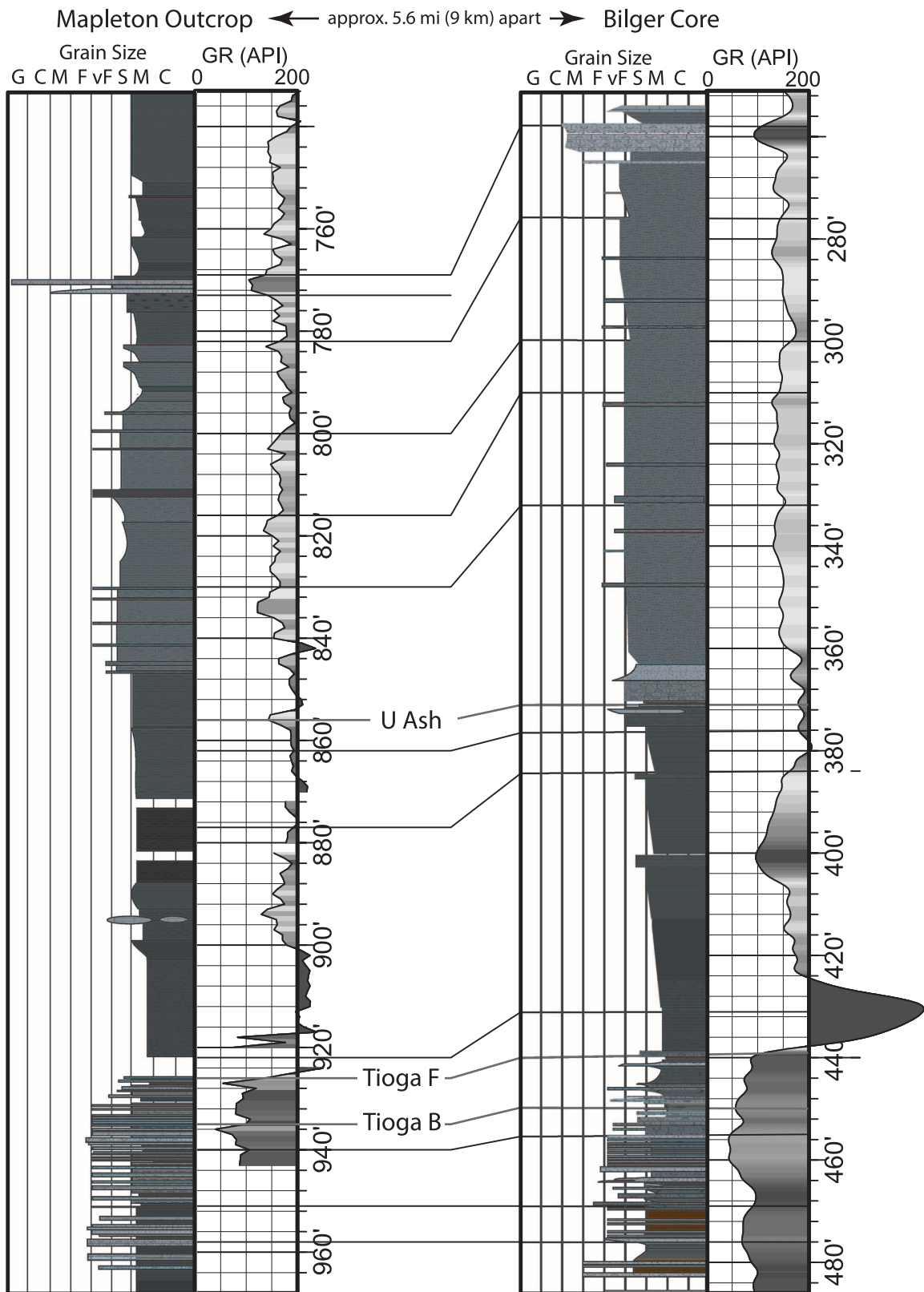
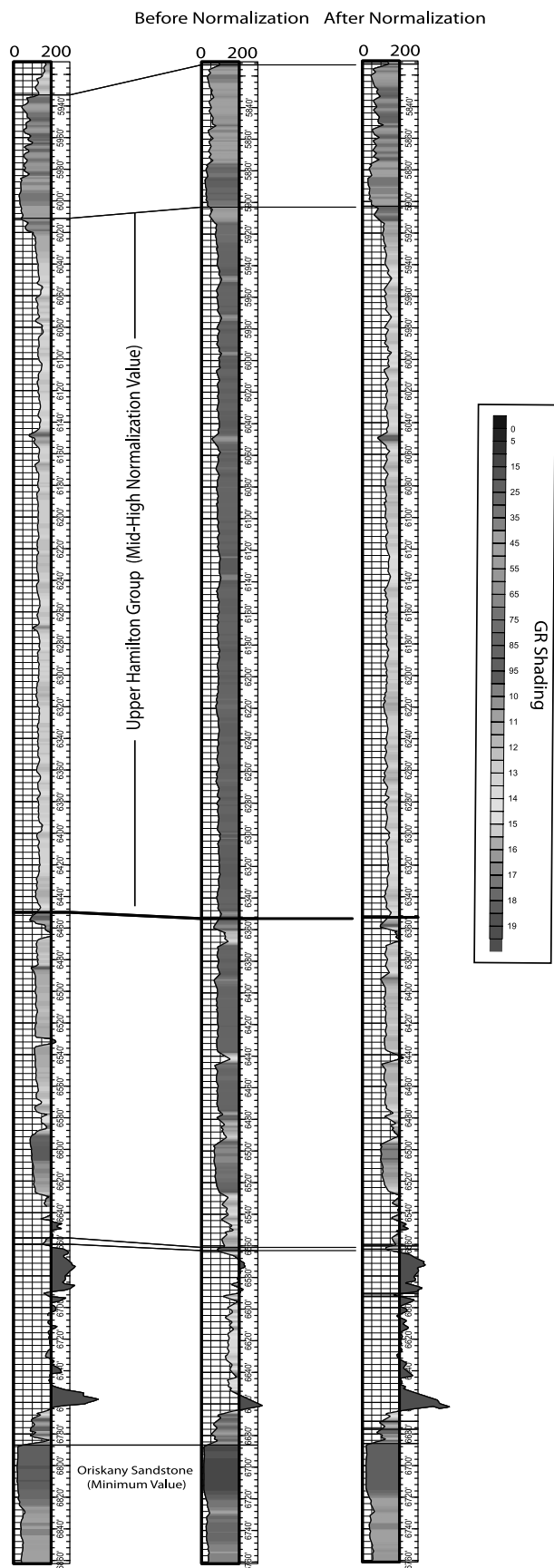


Figure 4. Lithic and gamma-ray (GR) logs from the Mapleton outcrop (site 3 in Figure 1) and the nearby Bilger core (site 4 in Figure 1) with suggested correlations. Similarities in GR logs demonstrate the effectiveness of handheld outcrop GR for aiding outcrop to subsurface correlations. Tioga B, F, and U ash are volcanic ashes correlatable across much of the basin. C = claystone; M = mudstone; S = siltstone; vF = very fine grained sandstone; F = fine-grained sandstone; M = medium-grained sandstone; C = coarse-grained sandstone; G = gravel.



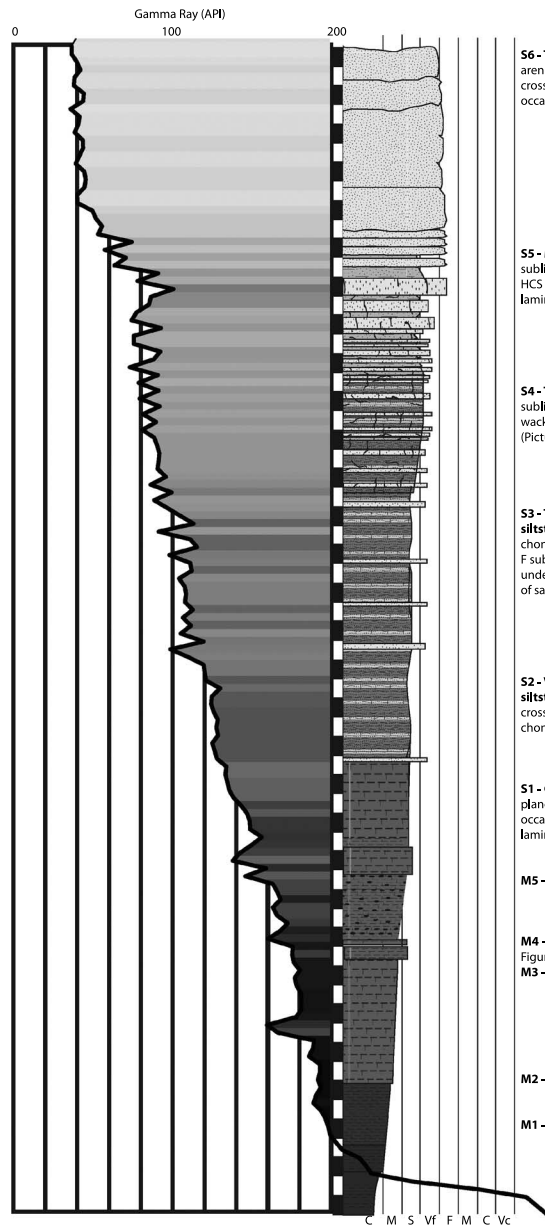
METHODS

Data Sets

Our data set includes 23 outcrops, 8 cores, and more than 1000 wireline well logs of the lower Kaskaskia supersequence throughout Pennsylvania and adjacent parts of New York, West Virginia, and Ohio (Figure 1). Although many different types of wireline logs were examined, correlations relied principally upon gamma-ray (GR) logs. At the 23 outcrops, we created standard lithic logs, and at 9 key sections, we measured GR profiles using a handheld spectral GR scintillometer (RS-230 BGO Super-Spec, Radiation Solutions). The scintillometer was placed on the outcrop face parallel to bedding, and measurements were taken every 6 in. (15 cm) using a 30-s assay time to produce a spectral GR log similar and comparable to wireline spectral GR logs (Figure 4; for discussion of technique, see Ettensohn et al., 1979; Chamberlain, 1984; Jordan et al., 1991; Svendsen and Hartley, 2001).

Eight cores were examined in this study, seven from shallow wells drilled near lower Hamilton Group outcrops in central Pennsylvania for the purpose of this study, and one from the Samson 1 Yoder well in the producing region donated by Samson Resources (Figure 1). Geochemical analyses for selected elements by ICP-AES (inductively coupled plasma atomic emission spectroscopy) and ICP-MS (inductively coupled plasma mass spectrometry) were performed on 1-in. (2.5-cm)-thick samples at 2-in. (5-cm) intervals from the entire Union Springs member in the Yoder-1 well core between 5627–5707 ft (1715–1739 m) depth. Organic- and carbonate-carbon from the same samples was analyzed by coulometry. Organic petrography, vitrinite

Figure 5. Results of gamma-ray (GR) log normalization for two closely spaced wells 2.18 mi (3.51 km) apart. COP Tract 16 12 is normalized using the log from well RW507 as the normalization standard with a low value from the Oriskany sandstone and a midhigh value from the mean GR in the upper Hamilton Group. The mean and standard deviation of 852 GR values from RW507 were 138 and 54 API, respectively. Before normalization, the mean and standard deviation of 1747 GR values from log COP Tract 16 12 were 95 and 37 API; after normalization, they were 139 and 54 API, respectively.



Facies Description

S6 - Thickly bedded clean sandstone. FV to F sublithic/quartz arenite, occasional thin shaley partings, common hummocky cross-stratification, occasional plane parallel laminations, occasional trough cross-stratification

S5 - Medium-to thickly bedded sandstone. FV to F sublithic/quartz arenite, interbedded with VF to F sublithic wacke, HCS common, some plane parallel laminations, some ripple laminations (Picture A)

S4 - Thin-to medium-bedded sandstone/wackestone. FV to F sublithic/quartz arenite. Interbedded with VF to F sublithic wacke, HCS common, some symmetrical ripple laminations (Picture B)

S3 - Thinly bedded sandstones interbedded with sandy siltstone. FV to F sublithic arenite, common planolites and chondrites bioturbation, some intervals are churned. Thin VF to F sublithic arenite sand beds, sand beds are sparse, differs from underlying facies in greater abundance and increased thickness of sand beds (Picture C)

S2 - VF to F sublithic arenite interlaminated with sandy siltstone. common ripple laminations and some hummocky cross-stratification on sand beds, occasional planolites and chondrites bioturbation (Picture D)

S1 - Calcareous sandy siltstone with thin sand laminations. plane parallel laminations are composed of very fine sand grains, occasional soft sediment deformation, occasional rippled laminations (Picture E)

M5 - Gray concretion-rich siltstone - See Figure 7

M4 - Calcareous siltstone with wackestone laminations - Figure 7

M3 - Laminated silty mudrock - See Figure 7

M2 - Black, faintly laminated, mudstone - See Figure 7

M1 - Black mudstone - See Figure 7

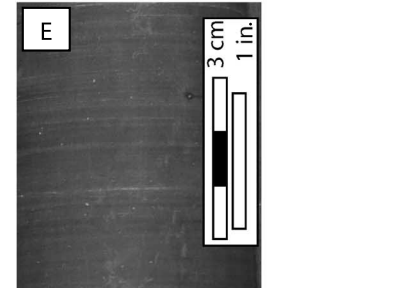
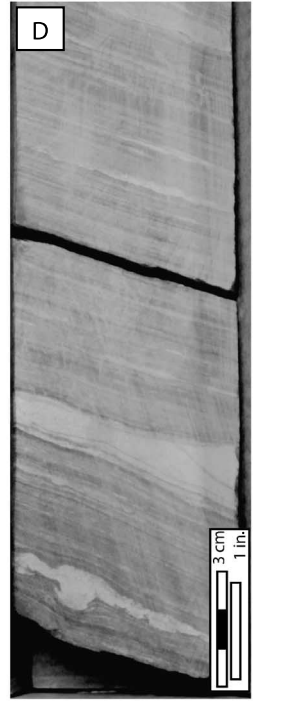
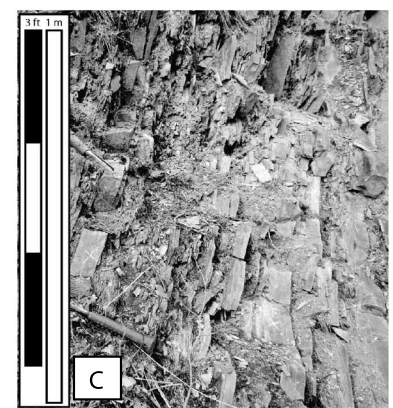
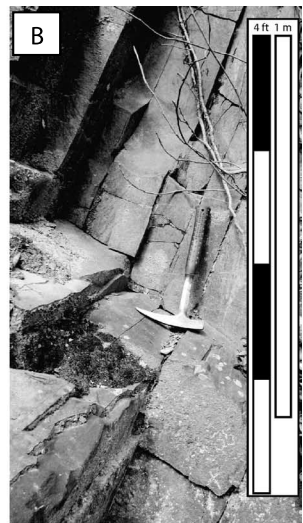


Figure 6. Standard siliciclastic-dominated facies progression and GR-log response. Grain sizes: C = claystone; M = mudstone; S = siltstone; vF = very fine grained sandstone; F = fine-grained sandstone; M = medium-grained sandstone; C = coarse-grained sandstone; Vc = very coarse grained sandstone. Facies M1–M5 are described in Figure 8. Vertical axis is tens to hundreds of feet. Photos: (A) facies S5 at East Waterford; (B) facies S4 at East Waterford; (C) facies S3 at East Waterford; (D) facies S2 in the Bilger core; (E) facies S1 in the Erb core.

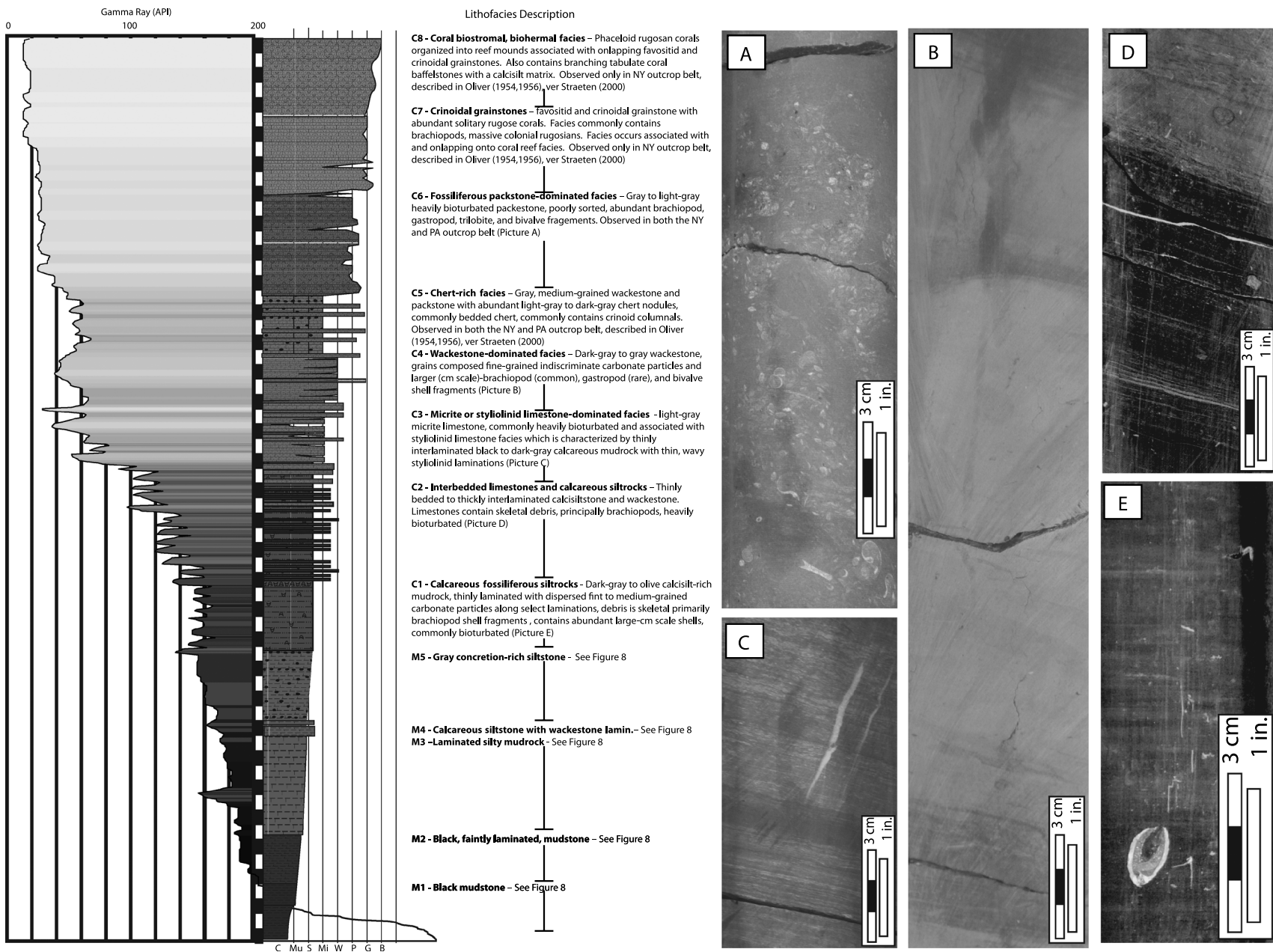


Figure 7. Standard carbonate-dominated facies progression and GR-log response. Grain-size abbreviations are defined in the caption of Figure 6. The vertical axis is tens to hundreds of feet. Photos: (A) facies C6 from Handiboe core; (B) facies C4 from Bilger core; (C) facies C3 from Bilger core; (D) facies C2 from Bilger core; (E) facies C1 from Erb core.

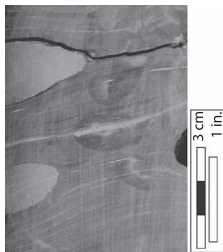
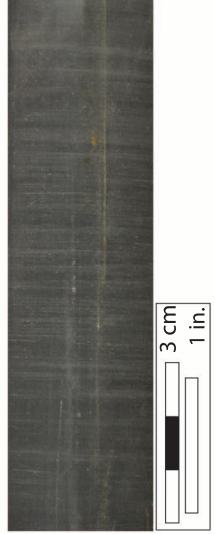
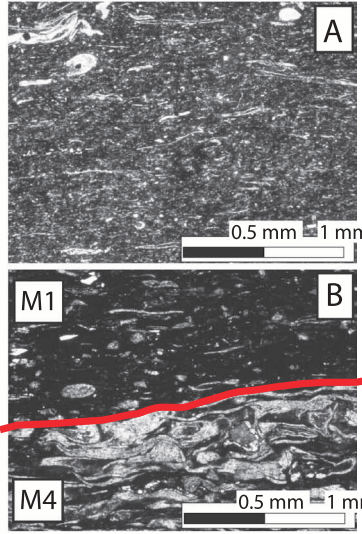
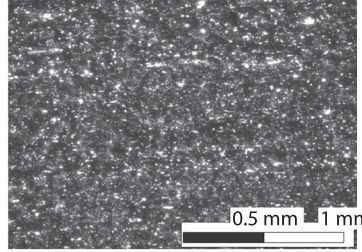
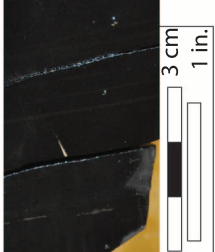
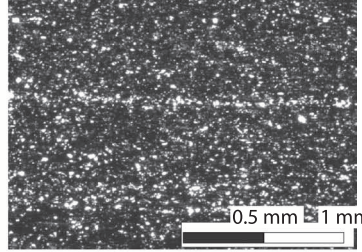
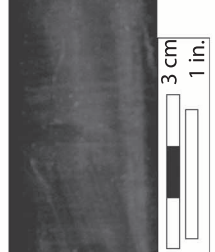
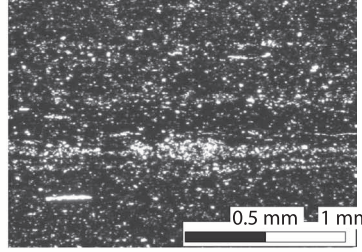
Facies	Core Photo	Thin Section Photo	Description
M5		No Thin Section	<p>Gray slightly calcareous siltstone, plane-parallel laminated with abundant concretions. Concretions are generally calcium carbonate. Plane-parallel laminations are generally contorted by differential compaction associated with concretions. Some laminations composed of very fine carbonate grains or pyrite nodules. Generally contains styliolinid- and <i>Tentaculites</i>-rich laminations.</p>
M4			<p>Dark-gray, calcareous siltstone, generally plane-parallel laminated with medium to very fine grained wackestone laminations containing, styliolinids, <i>Tentaculites</i>, and brachiopod shell fragments. Thickest laminations are lighter in color, composed of coarsest grains, and exhibit sharp to erosive bases that generally fine upward into more mud-rich laminations. Silt-sized grains are angular to subrounded and generally composed of calcium carbonate (20%–30% of bulk rock). Facies typically occurs associated with mudstone parasequence tops. Thin-section A shows typical M5 facies. Thin-section B shows mudrock parasequence top and sharp facies shift at the red line from M4 into M1.</p>
M3			<p>Dark-gray, silt-rich mudstone with thin to thick plane-parallel laminations. Pyritic (nodules and framboids), occasionally calcareous caused by very fine to silt-sized carbonate grain laminations, contains styliolinids and <i>Tentaculites</i> generally concentrated along laminations. Rock contains 50%–70% silt-sized grains and is dominantly composed of quartz. Bulk rock is 5%–10% calcium carbonate.</p>
M2			<p>Black mudstone with thin, faint, plane-parallel laminations. Pyritic (nodules and framboids) and generally containing quartz silt grains and occasional laminations. Contains styliolinids and <i>Tentaculites</i>. Mudrock composed of approximately 40%–50% silt-sized grains. Bulk rock is typically 4%–6% calcium carbonate.</p>
M1			<p>Black, organic-rich mudstone, massive to faintly laminated. Pyritic (nodules and framboids) and generally noncalcareous to slightly calcareous, styliolinids and <i>Tentaculites</i> occur in black mud matrix. Contains approximately 30%–40% silt-sized grains. Silt grains are angular to subrounded and composed of quartz. Bulk rock is typically 4%–6% calcium carbonate.</p>

Figure 8. Mudrock-dominated facies.

reflectance, and RockEval pyrolysis were conducted on a subset of these samples (Bracht, 2010).

Wireline GR well logs were collected from publicly available databases in Pennsylvania, New York, West Virginia, and Ohio. The older logs in the data set generally have narrower distributions skewed toward lower GR values when compared to nearby logs less than 20 yr old. This bias was corrected using a neighbor comparison and a scale-range high-low normalization as discussed in Shier (2004). The 872 older logs in the database were normalized to the nearest (surface distance) of the 146 modern GR logs using a low value obtained from the minimum GR value of the Oriskany sandstone or subjacent Helderberg Formation and a midhigh GR value defined by the mean GR value of the Mahantango Formation (Figure 5). We used a nearest-neighbor comparison because we observed significant and systematic changes in the GR values of the modern logs across the basin (particularly in the Mahantango Formation) and sought to preserve this variation as opposed to normalizing all logs to a common value.

Gamma-ray log response was mapped to lithofacies, generating simplified siliciclastic-dominated (Figure 6) and carbonate-dominated (Figure 7) GR signatures that were used to guide interpretation of mean GR responses in other wells. Mudstone-dominated rocks were divided into five facies (M1–M5) composed of mudstones to muddy siltstones with GR values in excess of 180° API (Figure 8). These facies represent the distal end members of both the siliciclastic- and carbonate-dominated systems. Six additional siliciclastic-dominated facies (S1–S6) were identified, ranging from siltstone with single-grain-thick sand laminations to dune trough cross-stratified sandstone. Five (C1–C5) of the eight carbonate-dominated facies were observed in central Pennsylvania cores. Carbonate facies (C6–C8) were observed only in New York, and their GR radioactivity was not directly measured; instead, outcrops were compared to nearby well logs.

Sequence Stratigraphy

This article uses the sequence-stratigraphic terminology, techniques, and approaches outlined in

Catuneanu (2006) and Catuneanu et al. (2009). Depositional sequences are composed of systems tracts that are further subdivided into parasequences. Parasequences are generally identified in GR logs by a GR decreasing-upward pattern culminating in a relatively abrupt shift to higher GR strata (Van Wagoner et al., 1990). Singh (2008) identified and described relatively small-scale parasequences within the Barnett Shale, noting that upward-decreasing GR trends observed in wireline logs corresponded to coarsening- or calcifying-upward lithologic changes in the organic-carbon-rich mudstones (Singh, 2008; Slatt and Abousleiman, 2011). Nearly identical GR patterns are observed in the Marcellus Formation and are used in this study to correlate well logs, cores, and outcrops.

Consistent with standard practice, we use parasequence stacking patterns to define systems tracts and depositional sequences. A retrogradational stacking pattern indicates that the accommodation rate (\dot{A}) exceeded the sedimentation rate (Q_s), and the parasequence(s) exhibiting this pattern represent the TST (Catuneanu, 2006). A normal regressive stacking pattern indicates Q_s exceeded \dot{A} , and this stratal package represents either the HST or LST (Catuneanu et al., 2009). A forced-regressive stacking pattern, characterized by a sharp basinward shift in facies and erosion of proximal strata, indicates a period of base-level fall ($\dot{A} < 0$), and strata deposited during this time are the FSST. Highstand systems tract and LST normal regressive stacking patterns are distinguished by an aggradational to progradational stacking pattern in the HST, and a progradational to aggradational stacking pattern in the LST (Neal and Abreu, 2009).

We also identify four key third-order sequence-stratigraphic surfaces: the sequence boundary (SB), maximum regressive surface (MRS), maximum flooding surface (MFS), and the basal surface of forced regression (BSFR). The SB is a surface of subaerial erosion combined with its correlative conformity (Catuneanu, 2006; Catuneanu et al., 2009) and is used to define the depositional sequences. The correlative conformity is defined as an approximation of the paleosea floor at the end of the forced regression and the onset of accommodation increase

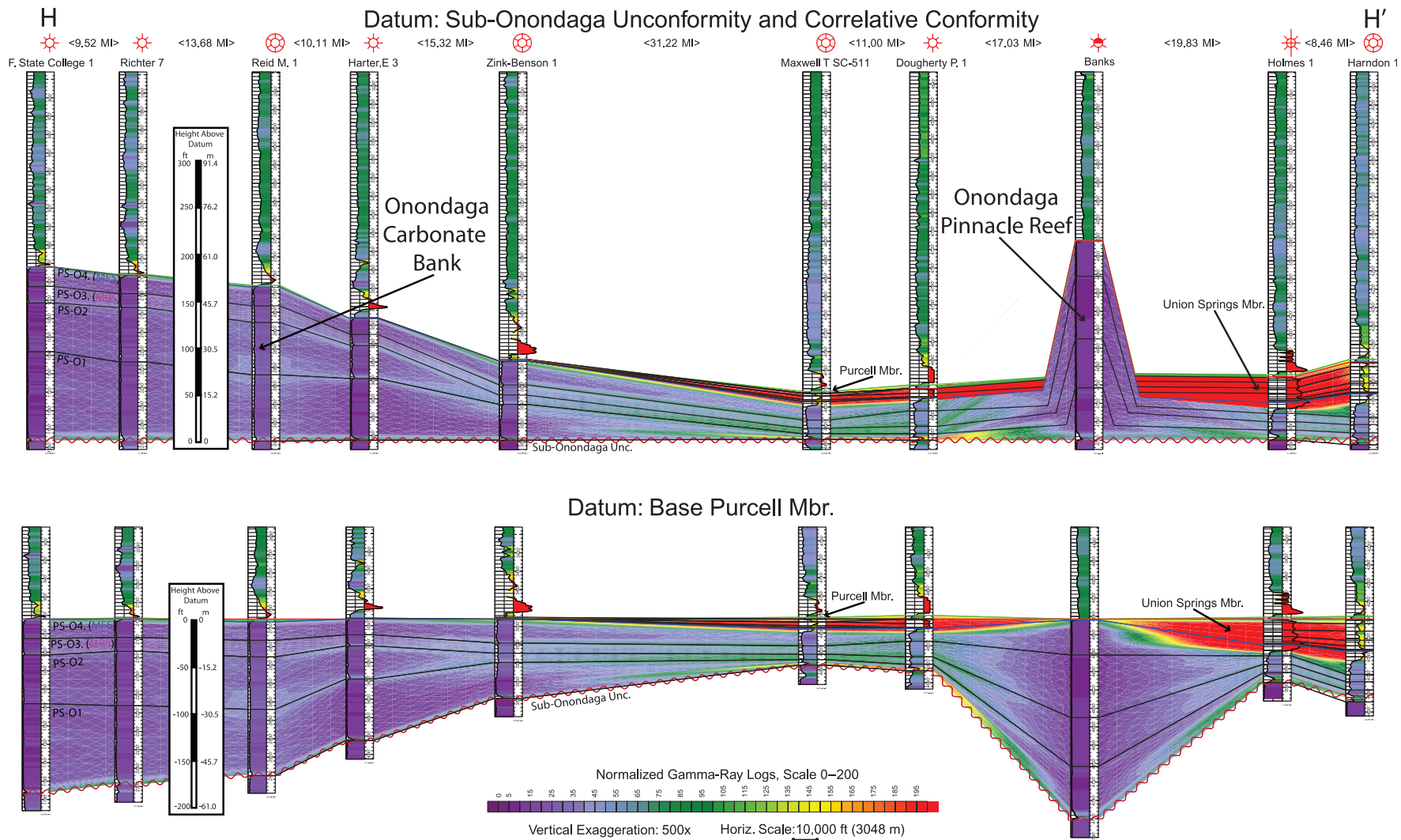


Figure 9. Correlation of line HH' using two different datums (see Figure 1 for line location). Upper correlation uses the sub-Onondaga unconformity as its datum and implies a minimum of 200 ft (61 m) of bathymetric difference between the western bank and pinnacle reefs and the basin floor at the end of deposition of the Onondaga Formation. Lower correlation hangs on the top of the Purcell Member (where preserved) and implies increased subsidence rates in the region of the western carbonate buildup. Using the sub-Onondaga unconformity as a datum is most consistent with interpreted facies (low-gamma-ray clean limestone to west grading into higher gamma-ray, more basinal facies to the east).

(Hunt and Tucker, 1992; Catuneanu, 2006). The MRS marks the change from shoreline regression to subsequent transgression and separates prograding strata from retrograding strata (Catuneanu, 2006). The MFS marks the landwardmost extent of the shoreline and a change from retrogradational to progradational strata (Posamentier and Vail, 1988; Van Wagoner et al., 1990; Catuneanu, 2006). As such, it indicates the end of transgression. The BSFR approximates the paleosea floor at the onset of base-level fall or regressive ravinement surface where subaqueous erosion occurred associated with the downward-shifting equilibrium wave profile (Hunt and Tucker, 1992; Catuneanu, 2006).

Choice of Datum

Some authors examining foreland systems place their datum on upper surfaces to demonstrate subsidence patterns. This study places the datum below the strata of interest on the sub-Onondaga unconformity because this surface produces more sensible thickness and facies distribution patterns in the upper Onondaga Formation (Figure 9). The sub-Onondaga unconformity also was used by Mesolella (1978) to examine Devonian and Silurian limestone paleogeography in the basin. Flattening on the sub-Onondaga unconformity requires that thick accumulations of relatively clean, low-GR, carbonate-bank limestone beds in the western parts of the basin grade eastward into thin, higher GR, more basinal facies deposited in deeper water. Not only is this interpretation consistent with paleowater depth interpretations of Onondaga Formation facies and sand redistribution patterns (Oliver, 1954, 1956; Brett and ver Straeten, 1994; ver Straeten and Brett, 1995; Wolosz, 1992), but it also aligns the tops of the tallest pinnacle reefs (approximately 200 ft [61 m] thick) lying to the east with the top of the carbonate bank to the west. Using an upper surface as a datum, such as the maximum marine flooding surface of the Union Springs member or the base of the Purcell Member, results in low GR, presumably deeper water carbonate facies of the Onondaga Formation deposited on a relative topographic high in the central part of the basin, and

coeval clean carbonate facies deposited in regions with higher accommodation to the west and to the east.

We acknowledge, however, that a datum on the sub-Onondaga unconformity or correlative conformity fails to account for any topography that likely existed on this surface, and it fails to account for the expected higher subsidence rates in the eastern part of the basin relative to the western part of the basin. In eastern parts of the basin, the sub-Onondaga unconformity represents significant erosion. Sandstone cobbles sourced from the Emsian Schoharie Formation and observed below the base of the Eifelian Onondaga Formation were transported southeastward as the unconformity was cut (ver Straeten and Brett, 2000; Brett et al., 2011). In the northwestern part of the basin (northwestern Pennsylvania, western New York), the sub-Onondaga unconformity is amalgamated with the Walbridge unconformity, placing the Eifelian Onondaga Formation directly on Early Devonian to Silurian strata (ver Straeten and Brett, 2000). In the central basin in Pennsylvania and New York, the Emsian–Eifelian contact is generally conformable. For these reasons, we hang one line on the top of the Purcell Member because in the region of that line, there appears to have been topography associated with the sub-Onondaga unconformity.

RESULTS AND INTERPRETATIONS

Onondaga Formation and Union Springs Member, Marcellus Formation: Parasequence Correlations

Ten parasequences have been identified in the Eifelian Onondaga Formation and Eifelian and Givetian Union Springs member of the Marcellus Formation (Figure 10). Three parasequences occur in the Onondaga Formation (PS-01, PS-02, PS-03), one parasequence spans the transition between the Onondaga Formation and the Union Springs member (PS-04), and six parasequences occur within the Union Springs member (PS-US1 to PS-US6). Figures 11 and 12 (foldout) contain seven cross

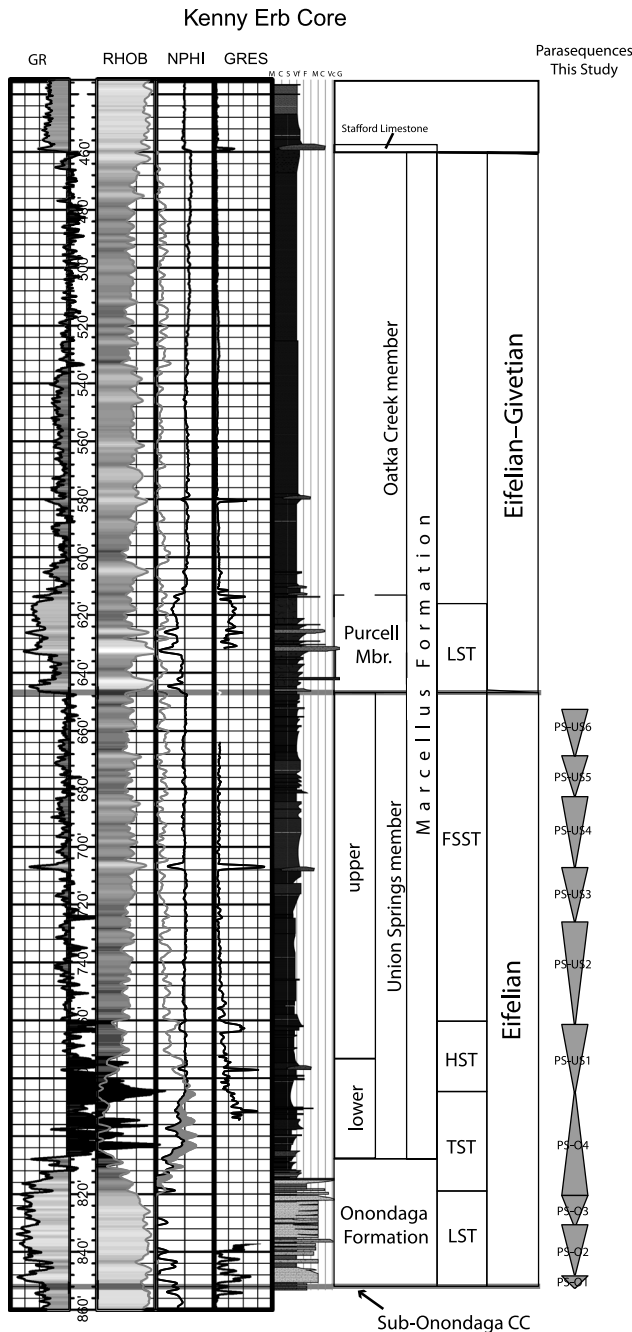


Figure 10. Wireline logs and graphic log from the Kenny Erb core (see Figure 1 for location). Depth is in feet. GR = Gamma-ray log (0° to 200° API); RHOB = Bulk density log (2.4 to 2.8 g/cm³); NPHI = neutron porosity log (0 to 0.2 v/v); DPOR = density porosity log (0 to 0.2 v/v); GRES = guard resistivity (0 to 1000 ohm m). Also shown is stratigraphic nomenclature used in this study for the Marcellus Formation and sequence-stratigraphic interpretations. Systems tracts and depositional sequence abbreviations are defined in the text.

sections that demonstrate parasequence correlations across the basin. Figure 11 highlights PS-01 to PS-04, and Figure 12 highlights PS-04 to PS-US6 (foldout). The Union Springs member is the most difficult to correlate because it shows the largest regional facies variation. Its parasequence correlations are somewhat interpretive, but are guided by a few key marker beds and GR log trends. The extent of PS-US1 is constrained by the overlying U ash. Parasequence PS-US2 is characterized by a blocky shape with a relatively sharp log and lithofacies shift that occurs near the U ash within this parasequence. Parasequence PS-US3 is capped by a carbonate concretion- or limestone-rich horizon that correlates to the *Cabrieroceras* bed identified by ver Straeten (2007). Overlying parasequences (PS4–PS6) are the most interpretive and are identified simply by correlating the first, second, and third parasequences above the PS-US3 top. Parasequence correlations are most difficult in the central parts of the basin where strata thin and exhibit higher GR values, presumably grading into the more distal mudrock-dominated facies (M1, M2) of the lower Union Springs member.

In central Pennsylvania, the first three Eifelian parasequences (PS-01, PS-02, PS-03) (Figure 10) start with sparsely bioturbated, black to dark-gray, calcareous siltstones that generally coarsen and calcify upward to fossiliferous, fine-grained, argillaceous wackestones. The parasequence-bounding marine flooding surfaces are characterized by a heavily bioturbated, fossiliferous packstone or by shell-hash layers that are overlain by slightly bioturbated to unbioturbated siltstones, indicating a sharp landward facies shift. Facies and ichnofaunal assemblages indicate a shoaling-upward pattern in each sequence with basal units that are populated by sparse *Chondrites*, middle units that are moderately bioturbated and contain *Chondrites* and *Planolites*, and upper facies that are heavily bioturbated and dominated by abundant large diameter (approximately 0.25 in. [0.5 cm]) burrows.

Parasequences PS-01, PS-02, and PS-03 thicken and generally decrease in GR value westward, northward, and northeastward, reflecting the change from the deeper water Selinsgrove Member of the Needmore Formation in central Pennsylvania to

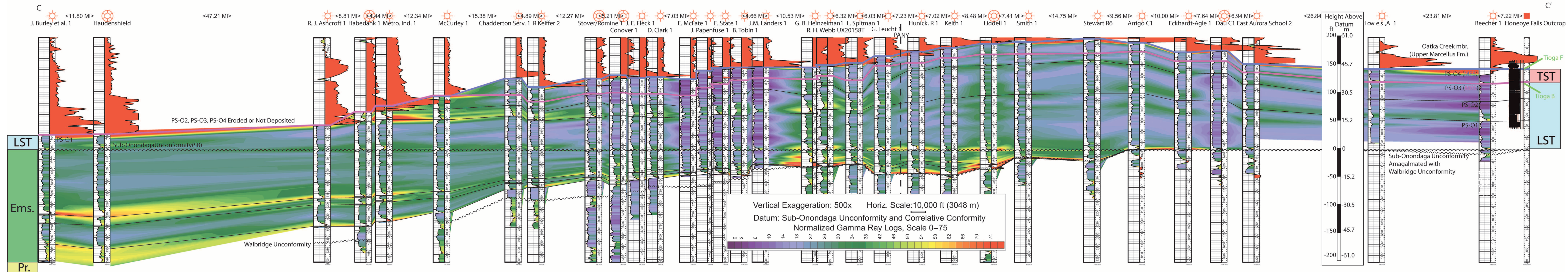
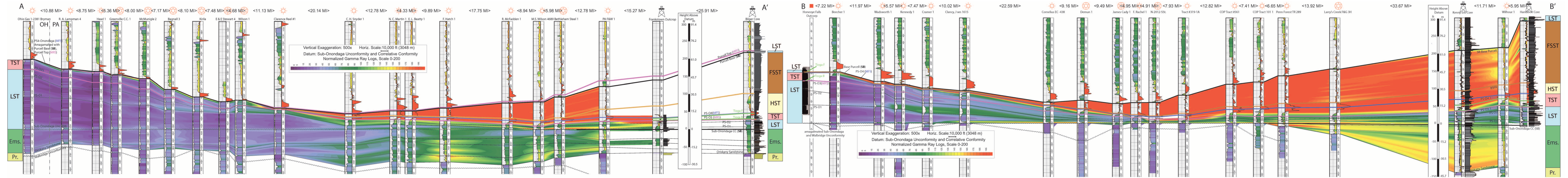


Figure 11. Correlated lines of section in the Onondaga Formation and lower Union Springs member (see Figure 1 for line locations). LST = lowstand systems tract; HST = highstand systems tract; FSST = falling-stage systems tract; TST = transgressive systems tract; CC = correlative conformity; Ems. = Emsian strata; Pr. = Pragian strata.

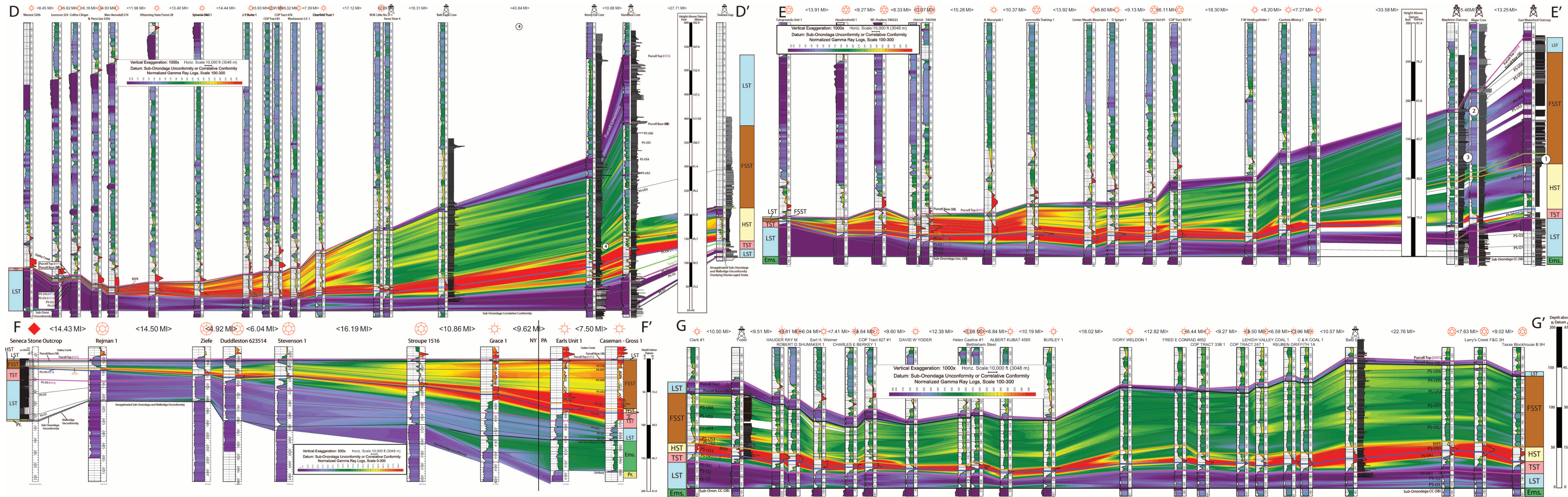


Figure 12. Correlated lines of section in the Union Springs and Purcell units, Marcellus Formation (see Figure 1 for line locations). LST = lowstand systems tract; HST = highstand systems tract; FSST = falling-stage systems tract; TST = transgressive systems tract; CC = correlative conformity; Ems. = Emsian strata; Pr. = Pragian strata.

shallower water facies of the Onondaga Formation (Figure 11 [foldout]) (also see Oliver, 1954, 1956; Inners, 1975; Wolosz, 1992; Brett and ver Straeten, 1994; ver Straeten and Brett, 1995). Correlations of wireline logs to sections in New York measured by ver Straeten (2007) indicate that the first parasequence (PS-01) is equivalent to the Edgecliff Member of the Onondaga Formation at that location (Wolosz, 1992; ver Straeten and Brett, 2000). The Edgecliff Member represents carbonate reefal or bank environments and grades eastward into deeper successional-mound and pinnacle-reef facies and ultimately into basinal facies in the center of the basin. The overlying parasequences (PS-02, PS-03) correlate with outcrops of the Nedrow and Moorehouse Members of the Onondaga Formation and represent a range of lithofacies including biostromal and biohermal coral facies and crinoidal grainstones, interbedded argillaceous limestones, and dark-gray calcareous shales (ver Straeten and Brett, 2000). The top of PS-02 correlates with the base of the Stroud bed discussed in ver Straeten (2007). The Stroud bed is a calcareous shale occurring above the PS-02 marine flooding surface. The Nedrow and Moorehouse Members exhibit a progradational stacking pattern from west to east across the New York outcrop belt (ver Straeten and Brett, 2000).

Parasequence PS-04 spans the transition from the Onondaga Formation to the Union Springs member. Unlike all other parasequences, PS-04 exhibits a fining-upward pattern, and bedsets exhibit a retrogradational stacking pattern. In central Pennsylvania, packstone and wackestone beds fine and thin upward and ultimately grade into the organic-carbon-rich mudrocks of the Union Springs member. Parasequence PS-04 contains seven of the Tioga Ash Beds, with Tioga B slightly above its base and Tioga F near its top. These ash layers allow a detailed chronostratigraphic correlation within PS-04 that indicates a retrogradational stacking pattern of coeval limestone overlain by organic-rich mudrock. In the central parts of the basin, GR values systematically increase upward in PS-04, and the parasequence top is placed at the highest GR, lowest bulk density value in the Union Springs member. In the northwest part of the basin where

this parasequence is thickest and the upper facies are interpreted to have been deposited in the shallowest water, the top of PS-04 is marked by a sharp flooding surface with a bone bed coarse lag and a sharp transition into the organic-rich mudrocks of the Union Springs member.

Six parasequences overlying PS-04 (PS-US1 to PS-US6) are identified in the Union Springs member (Figures 10, 12 [foldout]). Bedsets within these parasequences are generally thickest and exhibit lower GR values to the southeast. They thin and increase in GR values toward the basin center. Two lithologic units can be recognized in the Union Springs member in central Pennsylvania, here termed the lower and upper Union Springs member (Figure 10). The lower unit is characterized by black mudstones with approximately 10% total organic carbon (TOC), more than 50 ppm uranium, and 600°–800° API GR values. The upper unit, representing approximately the upper two-thirds of the member, is composed of silt-rich, and to the east sandy, mudstones with 1%–3% TOC and about 200° API GR. In central Pennsylvania, this lithologic division occurs approximately at the 1-in. (2.5-cm)-thick middle-Union Springs ash (U ash of ver Straeten, 2004).

Correlation of these parasequences, guided by the throughgoing U ash (within PS-US2), demonstrates that the upper Union Springs member is genetically related to the lower part of the Mahantango Formation (Figure 12 [foldout]). This relationship, first demonstrated locally in outcrops by ver Straeten (1996), indicates that the upper Union Springs member is a distal facies of the Mahantango delta complex, centered near Harrisburg, Pennsylvania (Mazzullo, 1973; Fail et al., 1978; Prave et al., 1996). In proximal outcrops (Figure 1, locations 5 and 9) the transition from organic-carbon-rich shale to thickly bedded sandstones is gradational, but occurs over a narrow stratigraphic interval (5–10 ft [1.5–3 m]) and, thus, represents a sharp basinward shift in facies and depositional environments. At medial outcrops and cores (Figure 1, locations 3 and 4), strata above the U ash are composed of predominantly thin sand beds intercalated with sandy siltstone (facies S1, S2, S3). These facies are nearly identical with

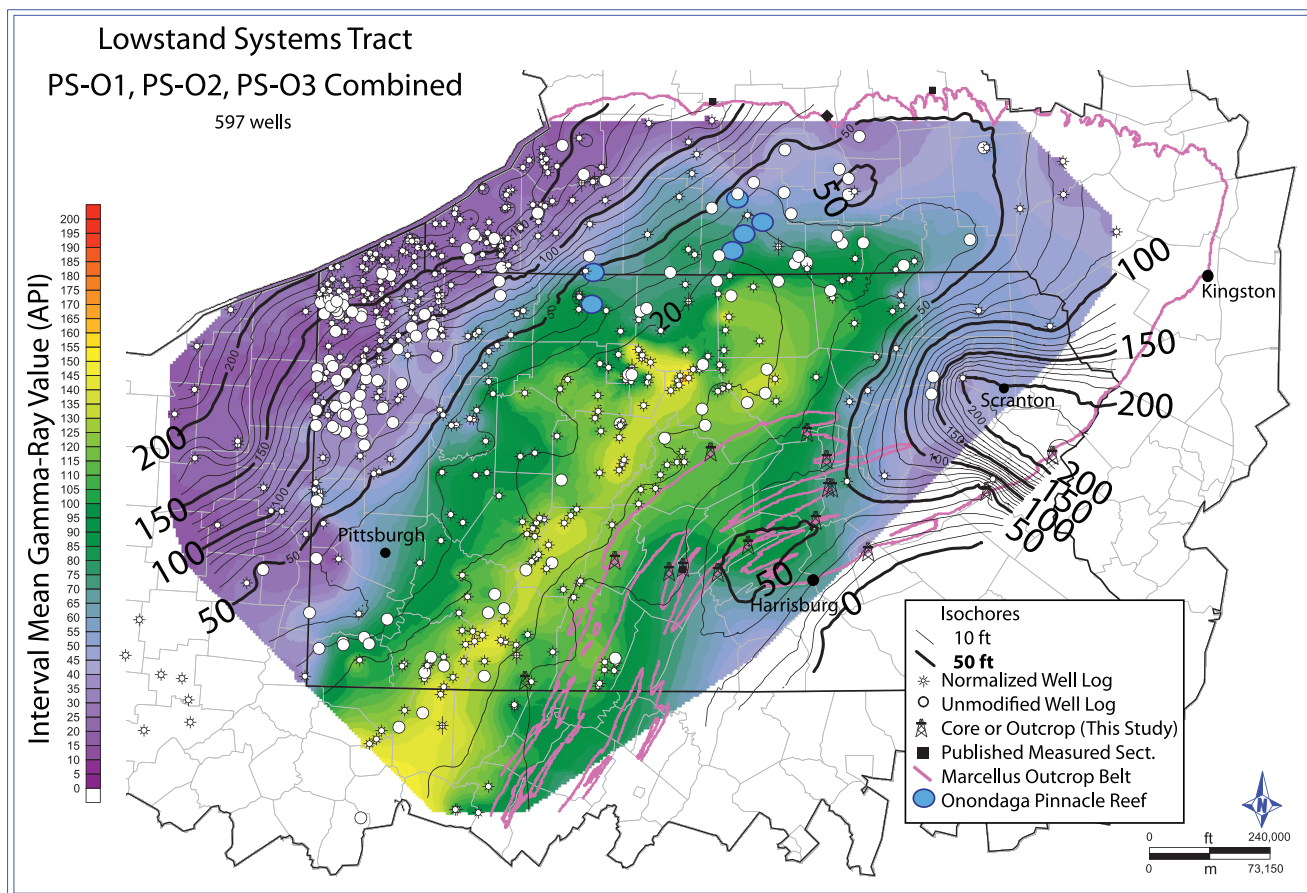


Figure 13. Mean gamma-ray and isochore thickness map of the lowstand systems tract which contains the first three parasequences in the Onondaga Formation (PS-O1, PS-O2, PS-O3). Thick (as much as 220 ft [67 m]), clean limestone accumulations in the northwestern and northern parts of the basin thin and grade argillaceous facies less than 20 ft (6 m) thick in the central, deeper part of the basin. A carbonate depocenter also exists to the east near Scranton, Pennsylvania.

the facies observed in the Stony Hollow Member at Kingston, New York (ver Straeten and Brett, 2006; ver Straeten, 2007). Above the U ash in more distal cores (e.g., Figure 1, locations 7 and 8) lies siltstone with thin, very fine grained, single-grain-thick sand laminations (facies S1, M6, M5, M4). Even more distal cores (Figure 1, locations 2 and 6) reveal mudrock-dominated facies and occasional carbonate concretions above the U ash. In west-central Pennsylvania, parasequences US1–US6 are composed of basal organic-carbon-rich mudstones (facies M1–M3) that generally coarsen or calcify upward (facies M3–M6), culminating in a shell-rich layer commonly dominated by tentaculites and styliolinids (Figure 8). These mudrock-dominated parasequence toes grade eastward and updip into coarser grained siliciclastic facies (Figure 12 [foldout], DD', EE').

Stratal Geometries and Depositional Environments of the Parasequences

Parasequences PS-O1 to PS-US6 comprise a single third-order depositional sequence (termed Eif) with PS-O1 to PS-O3 in the LST, PS-O4 in the TST, PS-US1 in the HST, and PS-US2 through PS-US6 in the FSST. This sequence-stratigraphic interpretation differs from Brett et al. (2011), who assigned the strata roughly equivalent to PS-O1 and PS-O2 to the Eif-1 depositional sequence and the strata roughly equivalent to PS-O3 and PS-US6 to the Eif-2 depositional sequence. Strata equivalent to Eif-1 and Eif-2 of Brett et al. (2011) are herein interpreted to represent a single third-order depositional sequence (Eif) with a duration of approximately 3 m.y.

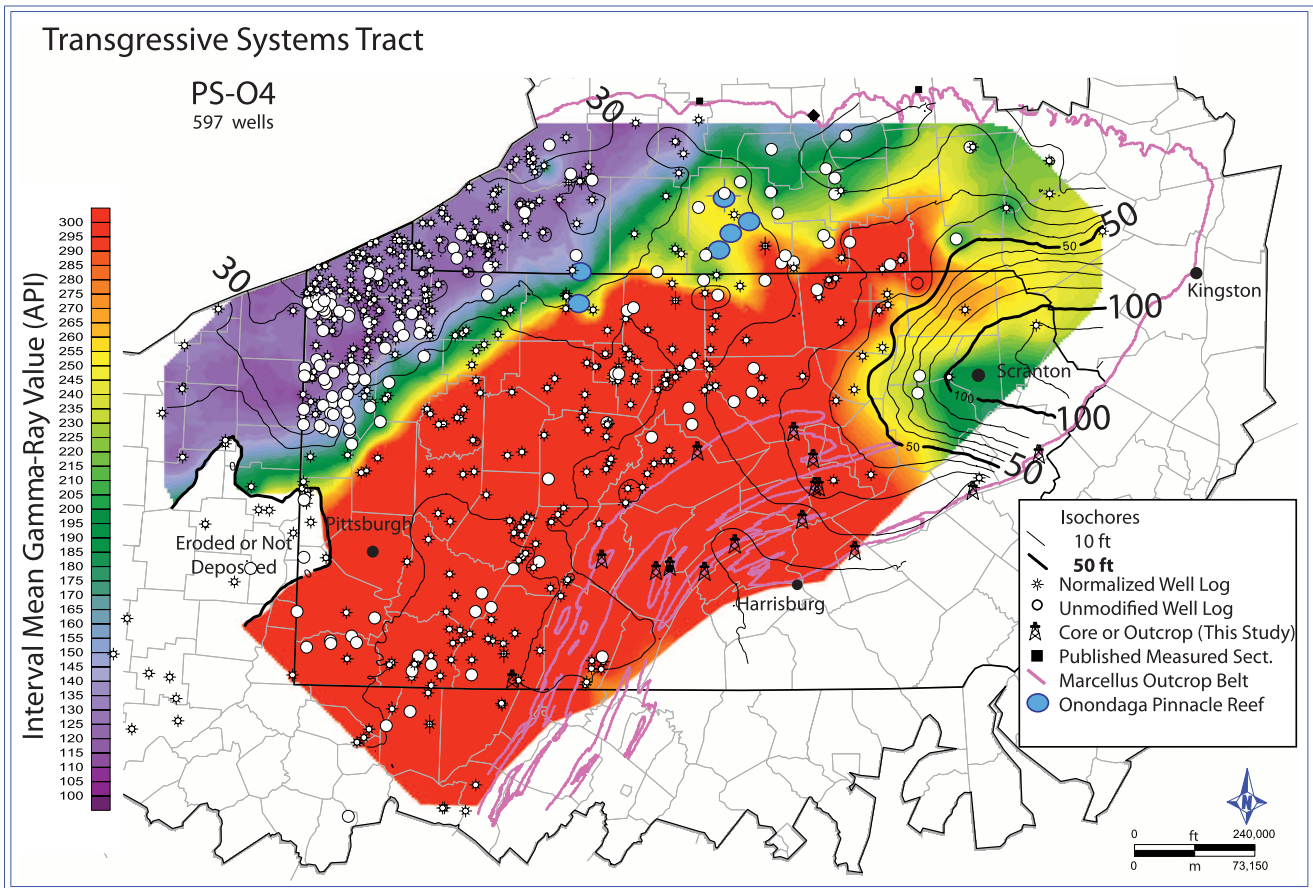


Figure 14. Mean gamma-ray and isochore thickness map of the transgressive systems tract, which is composed of the fourth parasequence in the Onondaga (PS-O4). The TST is characterized by relatively clean carbonates (as much as 30-ft [9-m] thick) in the western part of the basin and less than 10 ft (3 m) of organic-carbon-rich black mudrocks in the central, deeper parts of the basin. Like during the lowstand systems tract (Figure 13), a carbonate depocenter also exists to the east near Scranton, Pennsylvania.

Maps of parasequence thickness and GR-derived facies (Figures 13–17) provide a history of basin infilling. Gamma-ray values are mapped into facies using lithic logs from cores and Figures 6, 7, and 8. Parasequences PS-01 to PS-03 and PS-US3 to PSUS6 exhibit similar GR and isochore patterns and, therefore, are mapped and described together. Basal Onondaga Formation parasequences (PS-01 to PS-03) (Figure 13) are thickest and exhibit the lowest mean GR values in western Pennsylvania and New York. They thin and become more radiogenic eastward, culminating in a northeast-southwest trend across central Pennsylvania and New York. Pinnacle reefs occur along this trend where the sub-Onondaga unconformity completely removed the Emsian and, locally, Pragian strata (also see Rickard, 1984; ver Straeten, 1996; ver Straeten and Brett, 2000; Edinger et al., 2002). The

parasequences thicken again in eastern Pennsylvania and exhibit only medium GR values there. These trends are consistent with outcrop studies and reflect thick accumulations of clean, shallow-water limestones in the western and northeastern parts of the basin that grade into thin, argillaceous limestones and siltstones toward the central part of the basin.

Parasequences PS-01 through PS-03 are interpreted to arise during a period of base-level rise following formation of the sub-Onondaga unconformity. Their progradational to aggradational stacking pattern indicates that carbonate production rates were able to keep up with accommodation increase, and therefore, these strata comprise an LST. Thick, relatively clean carbonate accumulations in the northwest and north represent a large carbonate bank that rimmed the basin during the

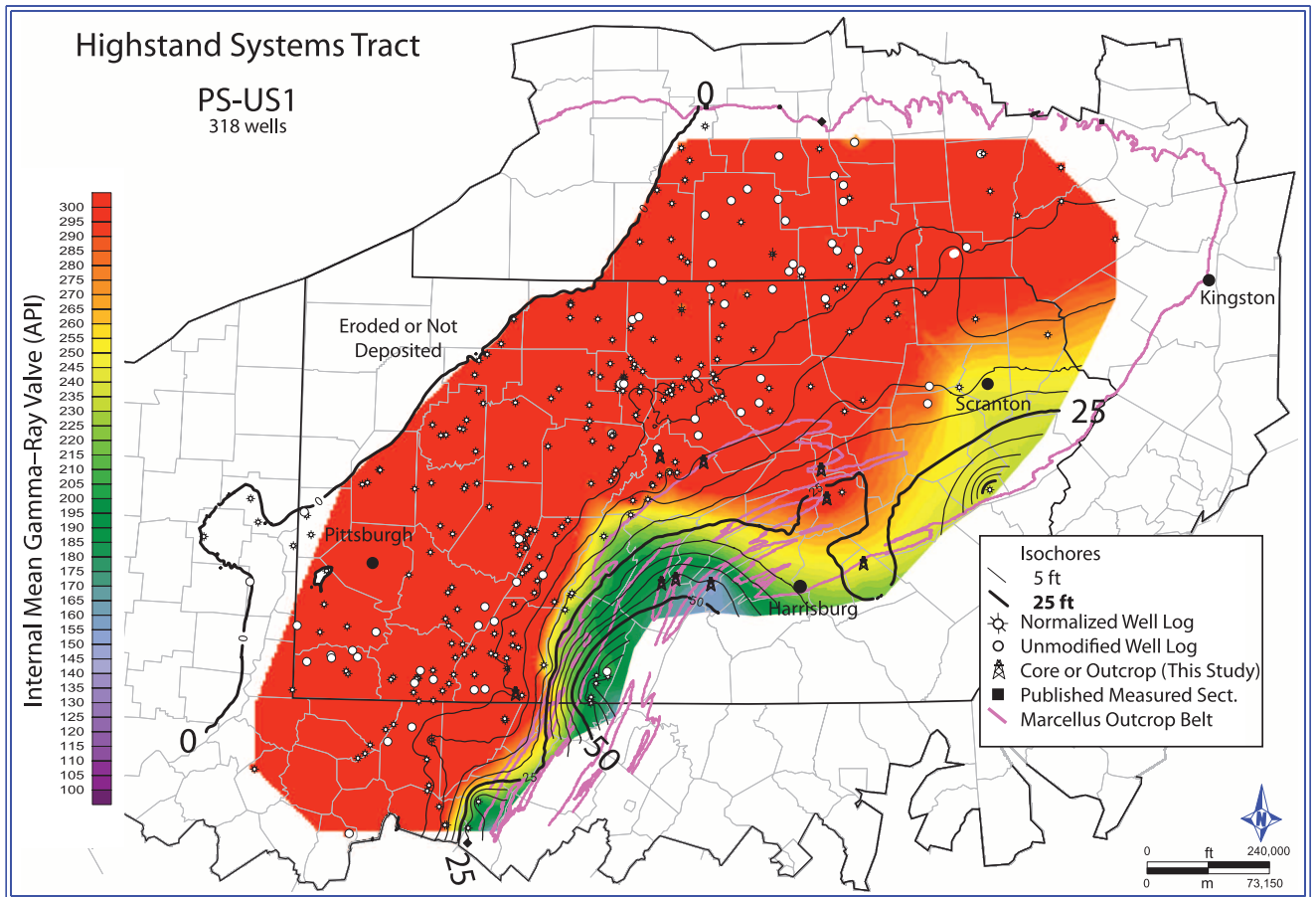


Figure 15. Mean gamma-ray and isochore thickness map of the highstand systems tract, which is composed of the first Union Springs member parasequence (PS-US1). A relatively low-GR lobate feature as much as 50 ft (15 m) thick exists west of Harrisburg, Pennsylvania. This is interpreted to be the result of clastic input into the basin from the highstand Mahantango delta complex. Strata thin generally to the northwest and pinch out in western Ohio, northeastern Pennsylvania, and western New York.

early Eifelian. Debris shed from this carbonate factory traveled to the deeper, central parts of the basin producing the finer grained, higher GR limestone facies observed there.

An isochore and mean GR map of PS-04 (Figure 14) coupled with outcrop and core facies descriptions indicate that this parasequence is dominated by moderately thick (as much as 50 ft [15 m]) accumulations of clean carbonates in the western part of the basin that rapidly grade eastward into more argillaceous carbonates and ultimately into organic-carbon-rich mudstones in the central part of the basin. Relatively lower GR values in the eastern part of the basin suggest additional carbonate input from the eastern and northeastern edges of the basin. The isochore maximum in northeastern Pennsylvania is composed of high

GR shales (>200° API) interbedded with argillaceous limestones (80°–120° API).

Parasequence PS-04 exhibits a generally fining-upward pattern, and bedsets exhibit a retrogradational stacking pattern, both interpreted to mean that carbonate production was unable to keep up with accommodation increase. Parasequence PS-04 represents a transgression, and these strata therefore are the TST. The maximum regressive surface defines the base of PS-04, slightly below the Tioga B ash, and the maximum flooding surface at the highest GR value in the Union Springs member defines the top. On the Onondaga carbonate bank in the north, PS-04 is truncated, and numerous shell hash horizons can be observed near the Onondaga Formation–Union Springs member contact. These hash beds are interpreted to be the flooding

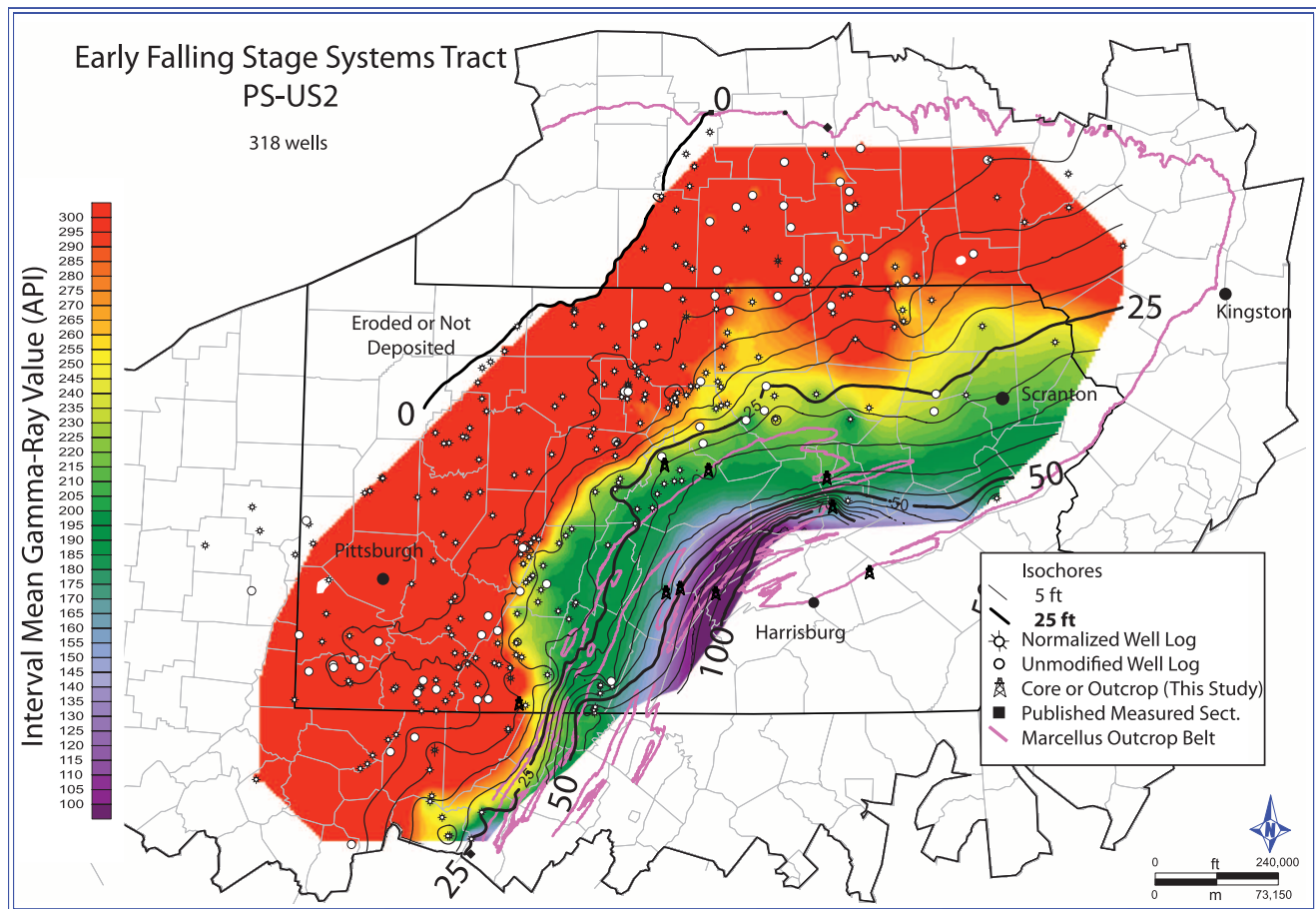


Figure 16. Mean gamma-ray (GR) and isochore thickness map of the early falling-stage systems tract, which is the second Union Springs member parasequence (PS-US2). Lobate GR and isochore feature observed in PS-US1 (Figure 15) shifts to the northwest. Strata are generally thicker in this interval, as much as 100 ft (30 m), and GR values are lower, indicating more influence from the Mahantango delta complex. Strata in this package pinch out along the same trend as PS-US1 (Figure 15).

surface at the top of PS-04. A complete TST is preserved in the central basin where the Onondaga Formation is thin.

A mean GR and isochore map of PS-US1 (Figure 15) shows a lobate feature west-southwest of Harrisburg, Pennsylvania, in both the isochore and mean GR. This feature reflects input of clastic material from the Mahantango delta. Isochore thicknesses likely reflect lateral infilling of bathymetric accommodation as well as higher subsidence rates associated with sediment- and thrust-load-induced subsidence.

During PS-US2, the locus of delta deposition shifted slightly to the north, and the delta complex prograded more to the northwest (Figure 16). This shift corresponds to the sharp basinward facies shift observed in proximal outcrops just below the

U ash within PS-US2 and is interpreted to be a forced regression caused by a period of base-level fall, and therefore, underlying strata (PS-US1) comprise the HST, and strata above the basal surface of forced regression are the FSST.

The thickness and GR patterns of PS-US3 through PS-US6, when combined, exhibit a continuation of progradation (Figure 17). In addition, a low-GR zone develops across central New York. This low-GR zone reflects the limestone-rich Union Springs member observed in that region and is interpreted to represent transport of carbonate material from the northwest. This interpretation is consistent with paleocurrent data in central New York in the overlying Purcell Member that indicate transport of material from the northwest to the southeast (Brett and ver Straeten, 1994;

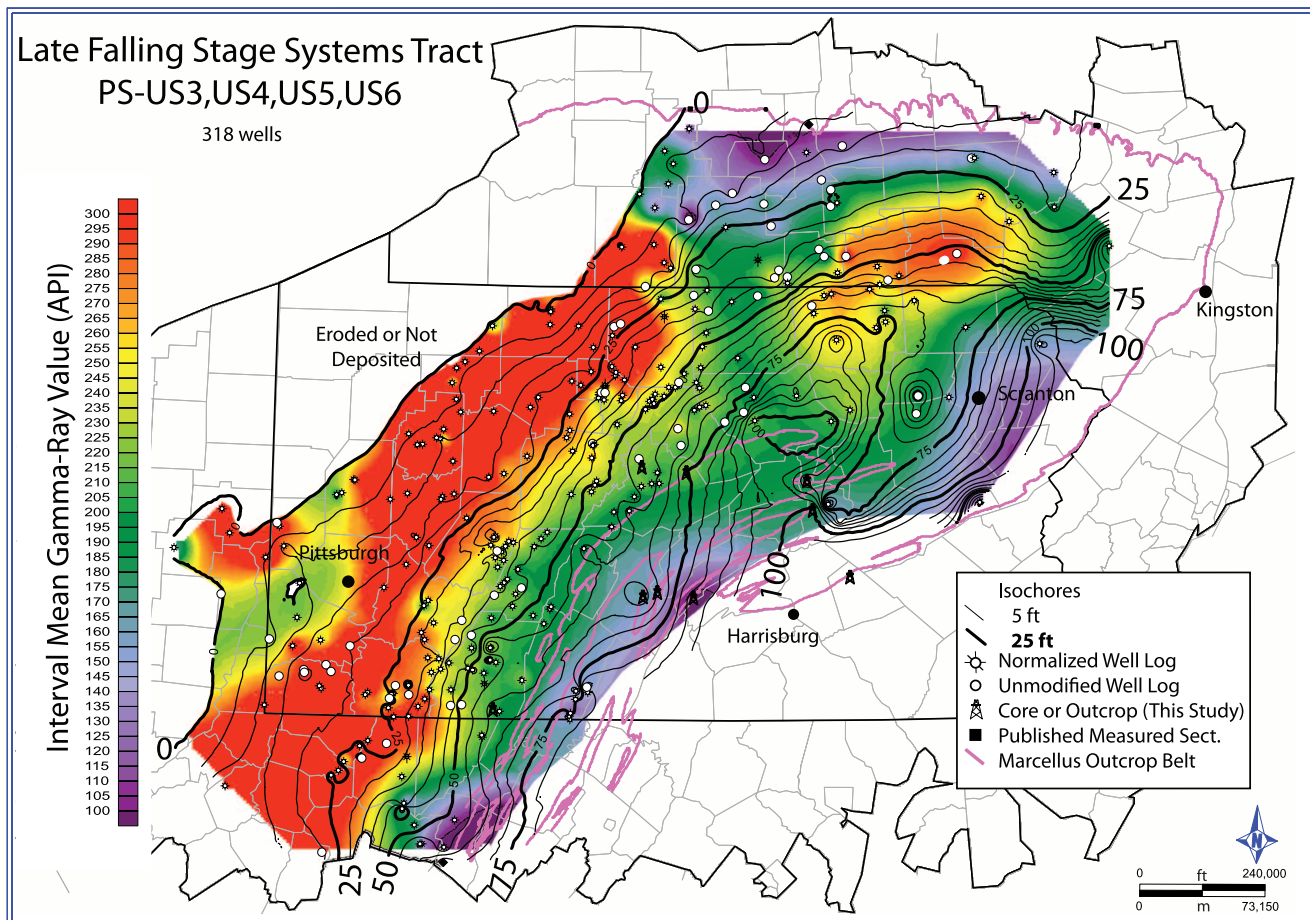


Figure 17. Mean gamma-ray (GR) and isochore thickness maps of the late falling-stage systems tract, which contains the third through sixth parasequence in the Union Springs member (PS-US3 through PS-US6). Base-level fall results in progradation of the delta complex. Relatively low GR values in New York suggest input of carbonate detritus from the northwest. Intermediate to high GR values around and west of Pittsburgh also suggest carbonate input from the Onondaga carbonate bank to the west. Strata are thickest, as much as 125 ft (38 m), in the east and thin to the north and northwest.

ver Straeten, 1995). The Union Springs limestones likely represent the earliest stages of local southeastward limestone progradation in central New York. Along the western pinch-out of the Union Springs member west of Pittsburgh, the mean GR values are only medium high (approximately 250° API), also suggesting carbonate input from the west. We include PS-US3 to PS-US6 in the FSST.

We interpret the western pinch-out of the Union Springs member parasequences to be caused by onlap onto the Onondaga Formation carbonate bank because trends of the pinch-out and the bank are similar and the subjacent strata of the bank increase in thickness there. This interpretation differs from Lash and Engelder (2011), who

interpreted a thin (<15 ft [<4.5 m]) Union Springs member throughout most of western Pennsylvania into eastern Ohio. Although it is possible that pockets of very thin (<5 ft [<1.5 m]) Union Springs lithologies are preserved in that region, the strata are discontinuous, and well-log facies are difficult to distinguish from the overlying Oatka Creek member. Outcrop observations in western New York and Ontario, Canada, demonstrate that the base of the overlying Purcell Member is erosive, with more than 3 ft (1 m) of relief and also locally directly overlies the Onondaga Formation (Brett and ver Straeten, 1994; ver Straeten, 1995; Brett et al., 2011). We interpret this erosion as a regressive wave ravinement (Catuneanu, 2006) associated with exposure of unlithified mudstones to storm and

potentially even fair-weather-wave base. No evidence has been reported supporting subaerial exposure of the Purcell Member or Onondaga Formation. In the northeastern corner of the basin, the relatively thick Onondaga Formation does not have a large effect on the thickness of the Union Springs member because of the higher subsidence rates there.

Taken together, Figures 13–17 document the evolving systems tracts of the central Appalachian Basin. Thickly to thinly bedded Mahantango Formation sandstones (GR, 40°–100° API; facies S6–S4; Figure 6) observed in most proximal outcrops are interpreted as a product of delta-top to delta-front depositional environments. These proximal facies grade basinward into a medial facies (GR, 100°–140° API; facies S3, S2; Figure 6) characterized by interlaminated sands and shales with local asymmetric ripple cross-laminated thin sand beds. The presence of asymmetric ripple laminations, load structures, and fining-upward beds suggests that thin sand beds were deposited by density-driven flows and likely were deposited at or below storm-wave base. Thin plane-parallel sand laminations (GR, 140°–160° API; facies S1; Figure 6) likely represent the distal toes of these density flows. Silt-rich mudstones (GR, 160°–190° API; facies M3–M5; Figure 8) were deposited farther down the clinoform face near the clinoform toe. The most organic-carbon-rich facies (GR >190°; facies M2–M1; Figure 8) was deposited on the basin floor. A modern analog for this facies progression is the Gulf of Papua clinothem off the southeast coast of Papua New Guinea (Slingerland et al., 2008a, b) where sands and organic-carbon-rich muds from five tropical rivers are prograding onto a carbonate shelf at the northern end of the Great Barrier Reef. Intercalated sands and shales are observed near the clinoform rollover and grade into a foreset dominated by organic-carbon-rich muds.

Geochemistry of the Union Springs Member

Visual analysis of organic matter (OM) throughout the Union Springs member in the Yoder-1 core indicates a primarily amorphous OM, and vitrinite

reflectance values average 2.25%. Pyrolysis hydrogen indices are less than 20 mg HC/g organic carbon, consistent with the relatively high thermal maturity of the unit. Key elements or ratios of elements that reflect changes in organic matter production, dilution, or oxidation (TOC %), redox conditions (Th/U, Fe_T/Al, Mo, Mn), and detrital components (K/[Mg + Fe], Ti/Al) are plotted in Figure 18.

The section starts with lower TOC values that correspond to limestone and marlstone beds in the transition from the underlying Onondaga Formation and rise to TOC values as high as 10 wt.%. The high TOC values appear to reflect preservation of organic matter under dominantly anoxic to euxinic bottom waters, as indicated by finely laminated, unbioturbated calcareous mudstone. The abundances of redox-sensitive elements strongly support this conclusion. Uranium (low Th and U values) and molybdenum concentrations are very high and are strongly positively correlated with one another and with TOC. The high U concentrations as revealed in spectral gamma-ray logs cause the strong gamma-ray signal (>550° API) in this interval. The Fe_T/Al ratios are high overall in PS-US1, corresponding to overall higher pyrite content. Pronounced peaks in Fe_T/Al are thin megascopic pyrite beds with abundant, small pyrite framboids. Studies of pyrite in sediments of the Holocene euxinic Black Sea (Wilkin and Arthur, 2001) indicate that much of the pyrite there was formed in the water column as framboids typically less than 12 μm in diameter. Molybdenum concentration in Black Sea sediments is commonly strongly correlated with TOC, and both are impacted by sediment dilution. However, Mo is more highly concentrated in deep-water masses and more readily sequestered in organic-carbon-rich sediments when those deep-water masses are euxinic (Tribovillard et al., 2006). Sequential extraction of euxinic Holocene Black Sea sediments indicates that a large proportion of the Mo resides in the sedimentary pyrite fraction. Thus, the predominance of framboids less than 12 μm and the extreme Mo enrichment in the Yoder-1 well core document a substantial euxinic (anoxic, sulfidic) water mass in the Middle Devonian Appalachian

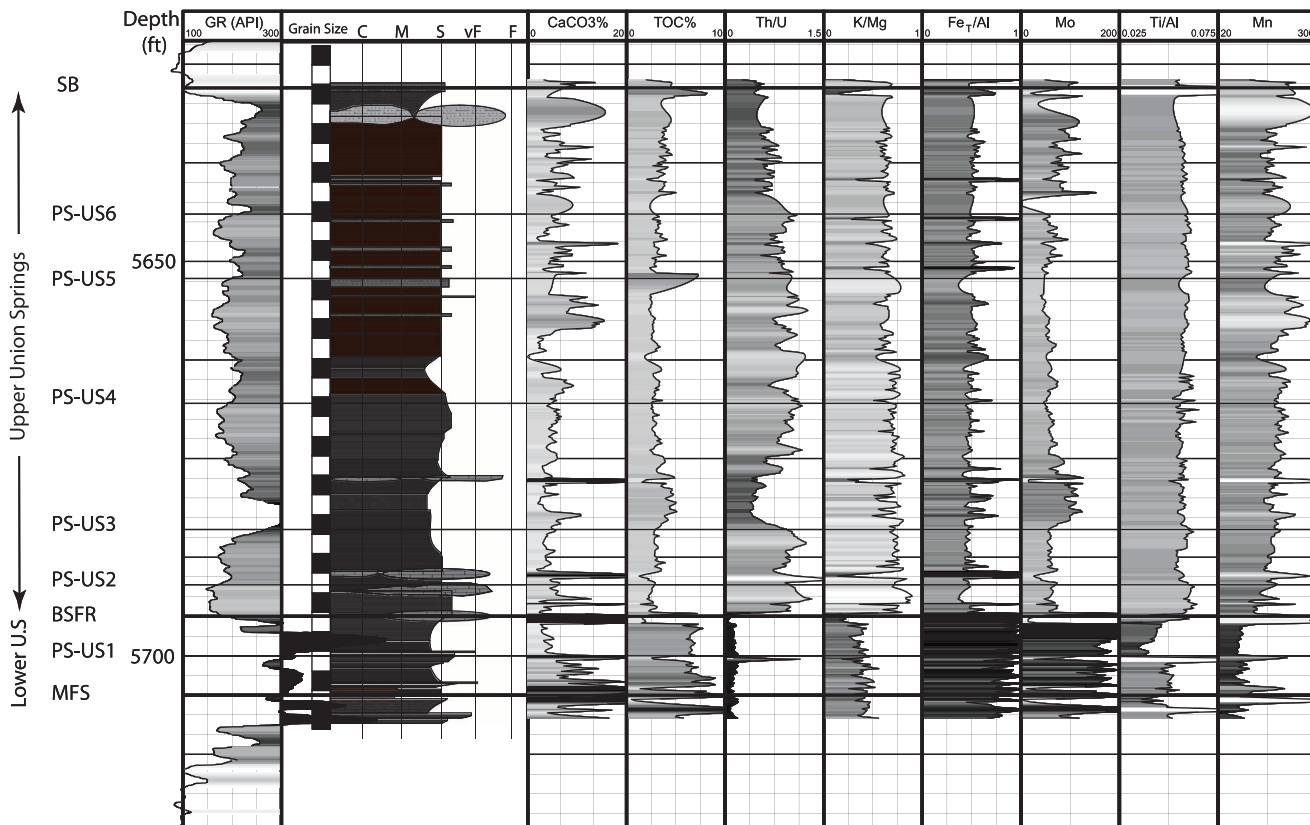


Figure 18. GR log, graphic log, and selected geochemical data from a core taken in the Samson 1 Yoder well, Somerset County (API: 37-111-20268). Geochemical data from Bracht (2010).

Basin, as was earlier proposed for many Upper Devonian black shales in the New York state part of the basin by Sageman et al. (2003; Arthur and Sageman, 2005). In addition, the low ratios of detrital indicators suggest low rates of clastic dilution during lower Union Springs member deposition. The low $K/(Mg + Fe)$ ratios suggest that clay mineral content is mostly mixed layer illite-smectite, not K-micas or pure illite (little K-feldspar exists as well), whereas the lower Ti/Al ratios suggest low amounts of detrital silt (such as rutilated quartz, titanomagnetite, etc.) in these shales. All of these parameters are consistent with a relative rise in sea level that trapped clastics to the east and carbonate detritus to the west.

At 5696 ft (1736 m) in the Yoder-1 well core, an abrupt shift in all the major parameters occurs at the U Ash and basal surface of forced regression. Although the silty mudstone of the Union Springs member remains predominantly finely laminated, the geochemical data indicate an ame-

lioration of the euxinic (sulfidic) conditions but persistence of anoxia at this site. The TOC, Fe_T/Al , and Mo concentrations decrease significantly, and Th/U increases. We interpret this Th/U increase to arise because Th-bearing clay fluxes increased as euxinic conditions waned; higher rates of sediment accumulation and lower rates of TOC accumulation decreased U fluxes to the sediment (e.g., Tribouillard et al., 2006), and therefore, U concentrations decreased relative to Th. A similar argument accounts for much lower Mo concentrations and a decrease in Fe_T/Al as well. The generally higher $K/(Mg + Fe)$ above 5696 ft (1736 m) is interpreted, along with the much higher Th/U values, as representing a greater proportion of K- and Th-bearing clay minerals as well as possible higher amounts of silt-size feldspar. The Ti/Al in that interval also is an indicator of increasing silt fraction, for example, as rutilated quartz and/or heavy minerals.

Several notable variations in Th/U, Mo, and TOC exist over the interval from 5696 to 5627 ft

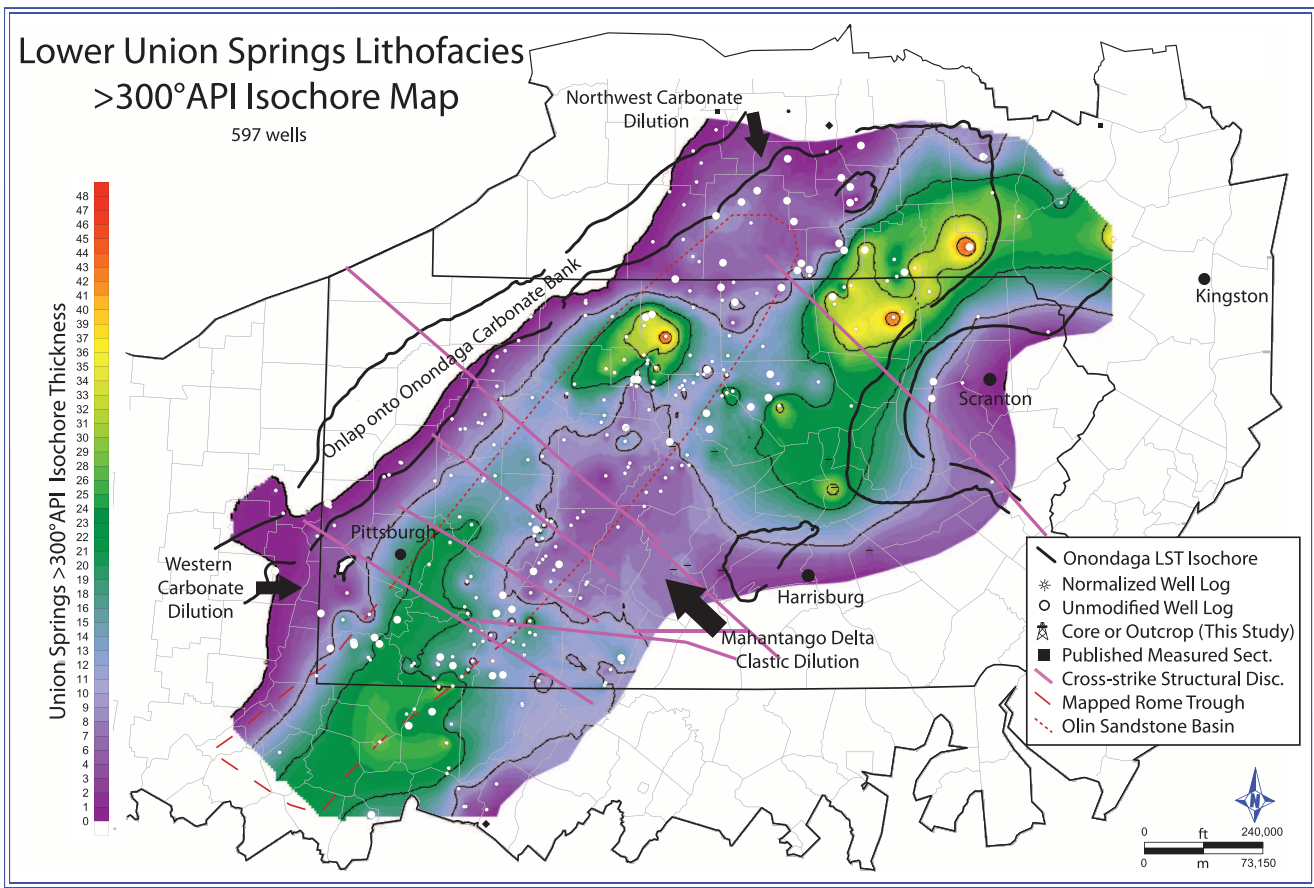


Figure 19. Net isochore map of lower Union Springs member with greater than 300° API. Three thicker high-gamma-ray regions are observed, one in southwestern Pennsylvania and West Virginia, one in north central Pennsylvania, one in northeast Pennsylvania and New York. Thickness patterns of this facies reflect onlap onto the Onondaga carbonate bank to the northwest and a facies change, caused by clastic dilution to the southeast.

(1736 to 1715 m) (upper Union Springs member) in the Yoder-1 core (Figure 18). The Th/U decreases, whereas the TOC and Mo concentrations increase in the lower parts of PS-US3 and through much of PS-US6, whereas variation in the clastic parameters is slight. This suggests short-term increases in intensity of anoxia during deposition of PS-US3 through PS-US6.

Over the entire Union Springs member, CaCO₃ ranges between 0% and 20% and occurs as thin, fossil-fragment-rich beds or concretions that are generally enriched in Mn and Fe. Most likely, Mn was incorporated in carbonate (concretions and cement) precipitated during early diagenesis in suboxic to anoxic conditions. Typically, in stratified anoxic basins, Mn²⁺ is not preserved in sediments because it is highly soluble. The exception occurs when high carbonate-ion concentrations

are present such that Mn²⁺ can substitute in the calcite lattice for Ca²⁺ ions of precipitated authigenic carbonates.

Summary

The thickest, high-GR (>300° API) Union Springs occurs in a generally northeast–southwest-trending belt across Pennsylvania (Figure 19). As indicated above, TOC and GR are strongly positively correlated, and therefore, we take Figure 19 to indicate the fairway of greatest TOC accumulation in the Eif-1 sequence. The origin of this fairway arises from a combination of causes. This was the region where bottom waters in the Appalachian Basin were dominantly euxinic during early Union Springs time of deposition, probably because it was deepest.

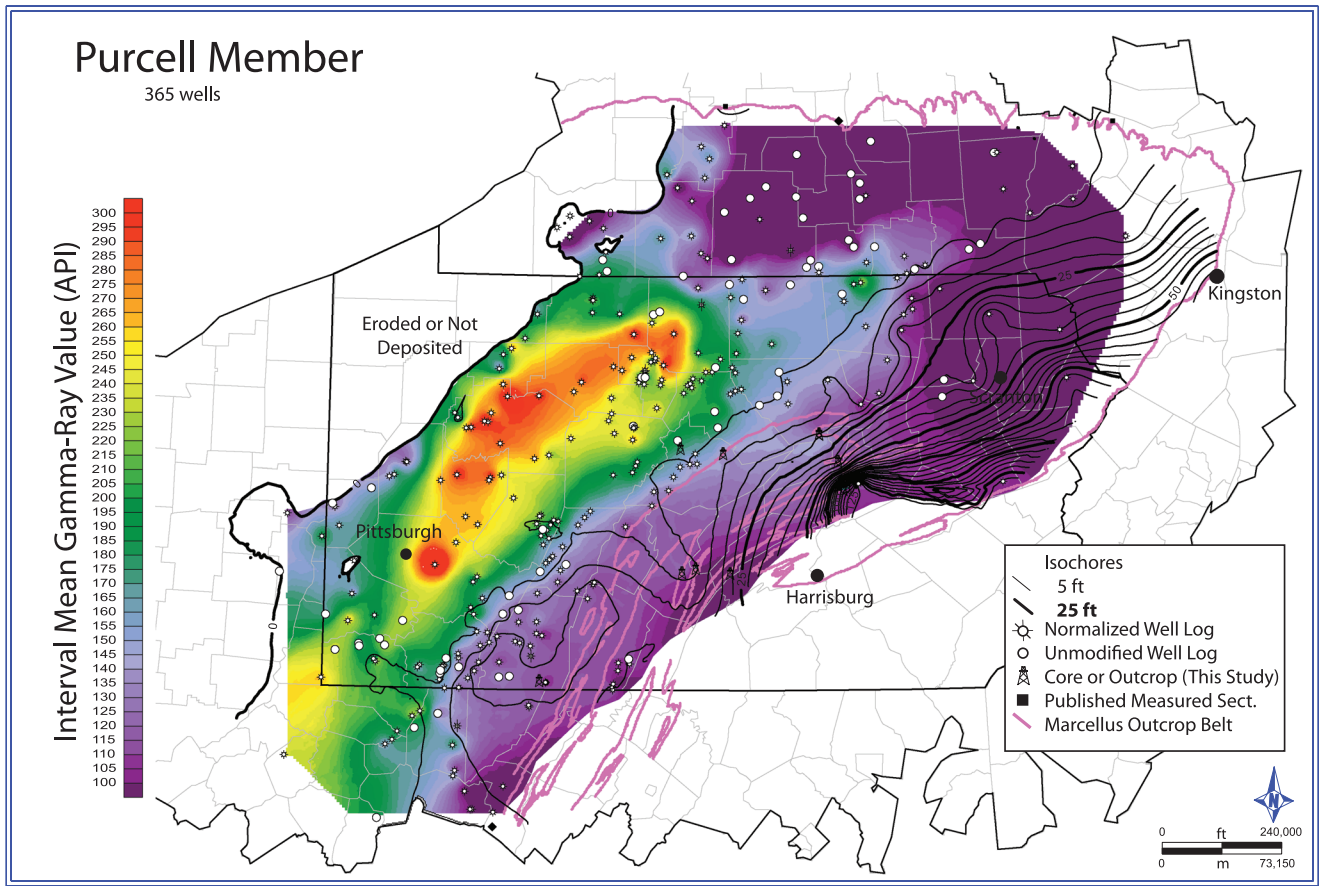


Figure 20. Mean gamma-ray (GR) and isochore map of the Purcell member. Thickest accumulations of limestone occur in the eastern and northern part of the basin in regions associated with the Mahantango delta complex and thick accumulations of the Onondaga Formation. High GR values in the central part of the basin suggest that black shale deposition was continuous during this time. In the northwesternmost parts of the basin, the Purcell Member onlaps onto the Onondaga carbonate bank.

It also was most distant from clastic sources of dilution to the east and carbonate sources to the west.

Purcell Member

The Purcell Member overlies the Union Springs member, except in the western parts of the study area where it sits unconformably on the Onondaga Formation or is not present. In central Pennsylvania, it consists of a 40-ft (12-m)-thick calcareous interval containing multiple limestone beds intercalated with marls and mudrocks that thin westward to about a 5-ft (1.5-m) interval of higher GR that is nevertheless still distinguishable on logs (e.g., Figure 12 [foldout]). To the east, the limestone facies grades into sandstone-dominated facies of the upper Turkey Ridge Sandstone member. The transitional facies is observed in central Pennsylvania

in the Bilger core and at the Mapleton outcrop (locations 4 and 3 in Figure 1), where the Purcell Member consists of a heavily bioturbated sandy limestone containing very fine- to coarse-grained, poorly sorted, angular to rounded quartz sand grains and occasional rounded quartz pebbles. The transition from the Union Springs member to the Purcell Member is generally sharp in the eastern parts of the study area, abrupt but gradational in the central parts, and erosive in the west. In contrast to the underlying unbioturbated Union Springs member, the Purcell Member from central Pennsylvania and eastward is generally bioturbated, exhibiting *Chondrites*, *Planolites*, and various larger burrows. However, in the Bald Eagle core, the Purcell Member is unbioturbated, suggesting a transition to poorly oxygenated conditions northwest and down the clinoform face.

A mean GR and isochore map of the Purcell Member (Figure 20) shows thick accumulations of low-GR sandstone and limestone-rich facies in the eastern parts of the basin that generally grade westward into higher GR more argillaceous facies toward the center of the basin. The western and northern parts of the basin also exhibit low mean GR values, indicating thin but relatively clean limestone deposits there. Mean GR values more than 300° API in the central part of the basin northwest of Pittsburgh indicate that deposition of organic-carbon-rich mudstone was continuous there (e.g., Figure 12 [foldout], DD', Kittanning State Forest 28).

In our interpretation, the Purcell Member comprises the LST to early TST of the Eifelian–Givetian depositional sequence of Brett et al. (2011). The mean GR pattern generally mirrors isochore and GR patterns in PS-US3 to PS-US6, suggesting that the previous basin bathymetry was inherited, and limestone deposition occurred where the bathymetry was shallower. We conjecture that an onset of accommodation increase during Purcell Member deposition sequestered clastic material in the east, proximal to the Acadian Mountains. Relatively shallow, oxygenated water in the east-central parts of the basin (as indicated by abundant bioturbation) was undiluted by clastic input, enabling widespread limestone deposition there. Limestone deposition kept up with rates of base-level rise, resulting in as much as 40 ft (12 m) of marl and limestone observed in the Handiboe and Roy Adams cores (Figure 11 [foldout]). Organic-carbon-rich mudstone deposition generally continued in the deeper parts of the basin (west-central Pennsylvania) during Purcell Member deposition. Continued base-level rise ultimately drowned out carbonate production and produced the generally retrogradational, backstepping facies associated with the lower parts of the Oatka Creek member (east Berne Member of the Mount Marion Formation in eastern New York; ver Straeten, 2007).

Controls on Base-Level Variation and Basin Depth

Various workers have proposed tectonically driven sequence development in the Middle Devonian

Appalachian Basin, arguing that stratal patterns resulted from thrust-induced subsidence or uplift, tectonic rebound, and/or bulge migration (Ettensohn, 1985; ver Straeten and Brett, 2000). Others have proposed models invoking eustatic and/or climatic forcing (Dennison and Head, 1975; Johnson et al., 1985; Bartholomew and Brett, 2007; ver Straeten, 2007). Most recently, Brett et al. (2011) revised the middle Devonian sea level curve and correlated Appalachian Basin sequences with coeval sequences in other North American intracratonic basins (Michigan, Illinois), thus arguing that eustasy and climate are the primary causes of the Middle Devonian sequences. Results presented here agree with Brett et al. (2011) that base-level fluctuations associated with the third-order Eifelian sequence likely were influenced by eustasy. As inferred from our systems tracts, base-level fluctuations appear to be synchronous on the proximal (east) and distal (west) sides of the basin, suggesting that thrust-load-induced tectonics was not the principal control. Apparent transgression during the TST is synchronous on the distal (northwestern) carbonate bank and to the east in the Acadian foredeep as evidenced by the thoroughgoing Tioga Ash Beds. Furthermore, base-level fall prior to deposition of the Purcell Member is necessary because the base is erosive in western parts of the basin and the sandstones observed in the foredeep bear the hallmarks of a forced regression. This pattern further supports accommodation increase in the southeast to eastern parts of the basin caused by thrust-load-induced subsidence. These observations are consistent with Brett et al. (2011), who observed coeval strata exhibiting similar apparent base-level fluctuations in the Michigan and Illinois Basins. The regional extent and duration (approximately 3 m.y.) of this Eifelian sequence suggest that base-level fluctuations were caused by eustasy or large-scale thermal uplift or subsidence superimposed over a continually subsiding basin. Eustatic fluctuations of this duration can be caused by processes such as changes in sea-floor spreading rate, global sedimentation, continental collision, or thermal subsidence and uplift of the Laurentian craton (Miller et al., 2005; Xie and Heller, 2009). Within the Eifelian depositional sequence lie seven parasequences representing base-level fluctuations

at approximately 400-k.y. intervals. A multitude of processes can explain these smaller base-level fluctuations, including climate variations resulting in changes in the clastic or carbonate sedimentation rates, global eustasy, or regional thermal uplift or subsidence.

Lash and Engelder (2011) argued that active basement structures, specifically the Rome trough and cross-strike structural discontinuities, controlled the distribution of the Marcellus Formation and associated strata. In their view, the basin could have been as shallow as 100–130 ft (30–40 m). Reactivation of basement faults produced regions of relatively higher basin topography, resulting in local sediment reworking and sediment starvation, ultimately producing the high GR and TOC facies observed in this central fairway. Note, however, that Rome trough basement faults are most prominent in southwest Pennsylvania and are inferred to continue throughout the northern parts of the state by thickness changes in the Cambrian Olin Sandstone (Kulander and Ryder, 2005). Figure 19 indicates that the region of thick, high GR Union Springs in southwestern Pennsylvania loosely correlates with the interpreted location of the Rome trough and Olin Basin. However, the geochemical interpretations and paleowater depth estimates in this study suggest a deep stratified water column, conflicting with the Lash and Engelder (2011) hypothesis. Syndepositional slip on Rome trough faults was not necessary to produce the observed stratal and facies patterns, but motion on these basement faults could act to increase basin bathymetry, producing even deeper water conditions in the Marcellus fairway.

We argue that the lower part of the Union Springs member was deposited in at least 330 ft (100 m) of deep water, but was likely deposited in much deeper water. At the end of deposition of the Onondaga Formation, 220 ft (67 m) of bathymetry existed in the basin. This was determined using the thickness differences between the Onondaga carbonate banks and pinnacle reefs and the thin, distal carbonate facies deposited in the central part of the basin (Figures 9, 13). Thrust-load-induced subsidence and preexisting topographic differences associated with the sub-Onondaga unconformity likely resulted in much greater bathymetric dif-

ferences because regions of thin Onondaga Formation deposits were located closer to the basin axis and over regions where the sub-Onondaga unconformity grades into its correlative conformity. Following the formation of the Onondaga carbonates, we interpret a significant transgression that resulted in the drowning of the bank and reefs and the deposition of organic-carbon-rich mudrocks associated with the lower Union Springs member. The relatively rapid drowning of carbonate reefs could have resulted from a combination of tectonic subsidence and eustatic sea level rise. Additionally, increased runoff from the Acadian Mountains could have resulted in lower salinity in surface waters and nitrification, which ultimately acted to limit platform carbonate production and allow drowning. Such processes could also aid in density stratification and an anomalously high organic matter production, resulting in a higher flux to the sediment. A more-than-110-ft (33-m) deepening of the basin would have produced a 330-ft (100-m)-deep central basin. This depth could have enabled water column stratification with euxinic bottom-water conditions. Following the deposition of the lower Union Springs member, base-level fall resulted in a forced regression, and the upper Union Springs member was deposited in more shallow water.

CONCLUSIONS

The Union Springs member of the Marcellus Formation and the Onondaga Formation compose a single third-order depositional sequence that spans most of the Eifelian. This depositional sequence comprises 10 parasequences (PS-01 through PS-04 and PS-US1 through PS-US6). The first three parasequences (PS-01, PS-02, PS-03) compose the LST. Parasequence PS-04 represents the TST, and PS-US1 represents the HST. Parasequences PS-US2 through PS-US6 compose the FSST, and the overlying Purcell Member comprises the LST of the next depositional sequence (Eifelian–Givefian).

The thickness and distribution of the facies associated with the Union Springs member and associated strata were controlled by base-level fluctuations

and topography inherited from the underlying Onondaga Formation. Prior to deposition of the Union Springs member, an Eifelian base-level rise prompted widespread limestone deposition represented by the Onondaga Formation. The thickest limestone accumulations occur in western and northern parts of the basin where preexisting Emsian topography resulted in shallow-water conditions that enabled limestone banks and reefs to keep up with the rate of accommodation increase. The carbonate banks grew to a height of approximately 220 ft (67 m) relative to the deeper central parts of the basin during this LST. Continued base-level rise drowned the Onondaga reefs and enabled water-column stratification and high-TOC mudstones of the TST to be deposited in the central, deepest (more than 330 ft [100 m] deep) parts of the basin. Subsequent base-level fall around the time of the deposition of the U ash caused a forced regression and a rapid progradation of clastic material from the east creating the FSST. Parasequence correlations aided by the throughgoing U ash indicate that some distal organic-carbon-rich facies in the central part of the basin are coeval with proximal forced regressive sandstones. The onset of base-level rise following upper Union Springs member and lower Mahantango Formation deposition sequestered clastic material to the east and enabled widespread limestone deposition of the Purcell Member on bathymetric highs in the basin.

The thickest accumulations of the most organic-carbon-rich Union Springs member occur in a northeast-southwest-trending fairway that is interpreted to be the deepest and most distal part of the basin. Water depths were sufficient to maintain euxinic conditions for hundreds of thousands of years. Organic-carbon-rich mudstones were deposited both as a hemipelagic basinal facies (TST, early HST) and as the distal toe of the prograding Mahantango delta clinof orm (FSST). A wide range of forcing mechanisms can be invoked to explain the facies distributions and sequence-stratigraphic relationships of the study interval. The larger third-order sequence (Eifelian) resulted from at least regional (North America) base-level fluctuations, suggesting that eustasy or thermal accommodation caused this sequence. Higher or-

der parasequences, especially PS-US1 through PS-US6, are less regionally extensive and may have been formed because of eustasy, climate, or local tectonics.

REFERENCES CITED

- Arthur, M. A., and B. B. Sageman, 2005, Sea-level control on source-rock development: Perspectives from the Holocene Black Sea, the mid-Cretaceous western Interior Basin of North America, and the Late Devonian Appalachian Basin, *in* N. B. Harris, ed., *Deposition of organic-carbon-rich sediments: Models, mechanisms and consequences: SEPM (Society for Sedimentary Geology) Special Publication 82*, p. 35–59.
- Bartholomew, A. J., and C. E. Brett, 2007, Correlation of Middle Devonian Hamilton Group-equivalent strata in east-central North America; implications for eustasy, tectonics and faunal provinciality; Devonian events and correlations, *in* R. T. Becker and W. T. Kirchgasser, eds., *Devonian events and correlation: Geological Society (London) Special Publication 278*, p. 105–131.
- Beaumont, C., G. Quinlan, and J. Hamilton, 1988, Orogeny and stratigraphy: Numerical models of the Paleozoic in the Eastern Interior of North America: *Tectonics*, v. 7, p. 389–416.
- Bracht, R., 2010, Geochemistry and depositional environment of the Union Springs Member of the Marcellus Shale in Pennsylvania: Master's thesis, The Pennsylvania State University, University Park, Pennsylvania, 60 p.
- Brett, C. E., 1998, Sequence stratigraphy, paleoecology, and evolution; biotic clues and responses to sea-level fluctuations: *Palaios*, v. 13, p. 241–262, doi:10.2307/3515448.
- Brett, C. E., and G. C. Baird, 1985, Carbonate-shale cycles in the Middle Devonian of New York: An evaluation of models for the origin of limestones in terrigenous shelf sequences: *Geology*, v. 13, p. 324–327, doi:10.1130/0091-7613(1985)13<324:CCITMD>2.0.CO;2.
- Brett, C. E., and C. A. ver Straeten, 1994, Stratigraphy and facies relationships of the Eifelian Onondaga Limestone (Middle Devonian) in western and west central New York state, *in* C. E. Brett and J. Scatterday, eds., *Field trip guidebook: New York State Geological Association 66th Annual Meeting Guidebook*, p. 221–269.
- Brett, C. E., G. C. Baird, A. J. Bartholomew, M. K. DeSantis, and C. A. ver Straeten, 2011, Sequence stratigraphy and a revised sea-level curve for the Middle Devonian of eastern North America: *Palaeogeography, Palaeoclimatology, Palaeoecology*, v. 304, p. 21–53, doi:10.1016/j.palaeo.2010.10.009.
- Castle, J. W., 2001, Appalachian Basin stratigraphic response to convergent-margin structural evolution: *Basin Research*, v. 13, p. 397–418, doi:10.1046/j.0950-091x.2001.00157.x.
- Catuneanu, C., 2006, *Principles of sequence stratigraphy*: Amsterdam, Elsevier, 345 p.
- Catuneanu, O., et al., 2009, Towards the standardization

- of sequence stratigraphy: *Earth-Science Reviews*, v. 92, p. 1–33, doi:10.1016/j.earscirev.2008.10.003.
- Chamberlain, A. K., 1984, Surface gamma-ray logs; a correlation tool for frontier areas: *AAPG Bulletin*, v. 68, p. 1040–1043.
- Coleman, J. L., R. C. Milici, T. A. Cook, R. R. Charpentier, M. Kirschbaum, T. R. Klett, R. M. Pollastro, and S. J. Schenk, 2011, Assessment of undiscovered oil and gas resources of the Devonian Marcellus Shale of the Appalachian Basin province: U. S. Geological Survey Fact Sheet 2011–3092, 2 p., accessed September 2013, <http://pubs.usgs.gov/fs/2011/3092>.
- Dennison, J. M., and K. O. Hasson, 1976, Stratigraphic cross section of Hamilton Group (Devonian) and adjacent strata along south border of Pennsylvania: *AAPG Bulletin*, v. 60, p. 278–287.
- Dennison, J. M., and J. W. Head, 1975, Sea-level variations interpreted from the Appalachian Basin Silurian and Devonian: *American Journal of Science*, v. 275, p. 1089–1120, doi:10.2475/ajs.275.10.1089.
- Desantis, M. K., C. E. Brett, and C. A. ver Straeten, 2007, Persistent depositional sequences and bioevents in the Eifelian (early Middle Devonian) of eastern Laurentia; North American evidence of the Kacak events?; Devonian events and correlations, in R. T. Becker and W. T. Kirchgasser, eds., *Devonian events and correlation: Geological Society (London) Special Publication 278*, p. 83–104.
- de Witt, W. Jr., J. B. Roen, and L. G. Wallace, 1993, Stratigraphy of Devonian black shales and associated rocks in the Appalachian Basin: *U.S. Geological Survey Bulletin*, v. 1909, p. B1–B47.
- Edinger, E. N., P. Copper, M. J. Risk, and W. Atmoyo, 2002, Oceanography and reefs of recent and Paleozoic tropical epeiric seas: *Facies*, v. 47, p. 127–150, doi:10.1007/BF02667710.
- Engelder, T. E., and G. G. Lash, 2008, Marcellus Shale play's vast resource potential creating stir in Appalachia: *The American Oil and Gas Reporter*, May 2008, v. 51, no. 6, p. 76–87.
- Epstein, J. B., 1984, Onesquethawan stratigraphy (Lower and Middle Devonian) of northeastern Pennsylvania: U.S. Government Printing Office, U.S. Geological Survey Professional Paper 1337, 35 p.
- Epstein, J. B., W. D. Sevon, and J. D. Glaeser, 1974, Geology and mineral resources of the Lehigh and Palmerton quadrangles, Carbon and Northampton counties: Pennsylvania Topographic and Geologic Survey, 4th Series, 460 p.
- Ericksen, M., D. Masson, R. Slingerland, and D. Swetland, 1989, Numerical simulation of circulation and sediment transport in the Late Devonian Catskill Sea, in T. A. Cross, ed., *Quantitative dynamic stratigraphy: Englewood Cliffs, New Jersey, Prentice-Hall*, p. 293–305.
- Ettensohn, F. R., 1985, The Catskill delta complex and the Acadian orogeny: A model, in D. L. Woodrow and W. D. Sevon, eds., *The Catskill delta: Geological Society of America Special Paper 201*, p. 39–49.
- Ettensohn, F. R., P. R. Fulton, and R. C. Kepferle, 1979, Use of scintillometer and gamma-ray logs for correlation and stratigraphy in homogeneous black shales: Summary: *Geological Society of America Bulletin*, v. 90, p. 421–423, doi:10.1130/0016-7606(1979)90<421:UOSAGL>2.0.CO;2.
- Fail, R. T., D. M. Hoskins, and R. B. Wells, 1978, Middle Devonian stratigraphy in central Pennsylvania; a revision: *Pennsylvania Geological Survey General Geology Report*, 28 p.
- Hunt, D., and M. E. Tucker, 1992, Stranded parasequences and the forced regressive wedge systems tract: Deposition during base-level fall: *Sedimentary Geology*, v. 81, p. 1–9, doi:10.1016/0037-0738(92)90052-S.
- Inners, J. D., 1975, The stratigraphy and paleontology of the Onesquethaw stage in Pennsylvania and adjacent stages: Ph.D. thesis, Amherst, University of Massachusetts, 666 p.
- Johnson, J. G., G. Klapper, and C. A. Sandberg, 1985, Devonian eustatic fluctuations in Euramerica: *Geological Society of America Bulletin*, v. 96, p. 567–587, doi:10.1130/0016-7606(1985)96<567:DEFIE>2.0.CO;2.
- Jordan, D. W., R. M. Slatt, R. H. Gillespie, A. E. D'Agostino, and M. H. Scheihing, 1991, Applications of outcrop gamma-ray logging to field development and exploration: Reservoir characterization: Petrophysical formation evaluation and rock description, in R. Sneider, W. Massell, R. Mathis, D. Loren, and P. Wichmann, convenors, *The integration of geology, geophysics, petrophysics and petroleum engineering in reservoir delineation, description and management: AAPG Special Publication 26*, p. 104–122.
- Kaufmann, B., 2006, Calibrating the Devonian time scale: A synthesis of U-Pb ID-TIMS ages and conodont stratigraphy: *Earth Science Reviews*, v. 76, p. 175–190, doi:10.1016/j.earscirev.2006.01.001.
- Kulander, C. S., and R. T. Ryder, 2005, Regional seismic lines across the Rome trough and Allegheny Plateau of northern West Virginia, western Maryland, and southwestern Pennsylvania: *U.S. Geological Survey Geologic Investigations Series Map I-2791*, 9 p.
- Lash, G., and T. Engelder, 2011, Thickness trends and sequence stratigraphy of the Middle Devonian Marcellus Formation, Appalachian Basin: Implications for Acadian foreland basin evolution: *AAPG Bulletin*, v. 95, p. 61–103, doi:10.1306/06301009150.
- Mazzullo, S. J., 1973, Deltaic depositional environments in the Hamilton Group (Middle Devonian, southeastern New York state): *Journal of Sedimentary Research*, v. 43, p. 1061–1071, doi:10.1306/74D728F1-2B21-11D7-8648000102C1865D.
- McCullum, L. B., 1988, A shallow epeiric sea interpretation for an offshore Middle Devonian black shale facies in eastern North America, in A. F. Embry and D. J. Glass, eds., *Devonian of the world II: Canadian Society of Petroleum Geologists Memoir 14*, p. 347–355.
- Mesoella, K. J., 1978, Paleogeography of some Silurian and Devonian reef trends, central Appalachian Basin: *AAPG Bulletin*, v. 62, p. 1607–1644.
- Milici, R. C., and C. S. Swezey, 2006, Assessment of Appalachian Basin oil and gas resources: Devonian shale—Middle and upper Paleozoic total petroleum system: *U.S. Geological Survey Open-File Report 1237*, 54 p.

- Miller, K. G., M. A. Kominz, J. V. Browning, J. D. Wright, G. S. Mountain, M. E. Katz, P. J. Sugarman, B. S. Cramer, N. Christie-Blick, and S. F. Pekar, 2005, The Phanerozoic record of global sea-level change, *Science*, v. 310, no. 5752, p. 1293–1298.
- Neal, J., and V. Abreu, 2009, Sequence stratigraphy hierarchy and the accommodation succession method: *Geology*, v. 37, p. 779–782, doi:10.1130/G25722A.1.
- Oliver, W. A., 1954, Stratigraphy of the Onondaga Limestone (Devonian) in central New York: Geological Society of America Bulletin, v. 65, p. 621–652, doi:10.1130/0016-7606(1954)65[621:SOTOLD]2.0.CO;2.
- Oliver, W. A., 1956, Stratigraphy of the Onondaga Limestone in eastern New York: Geological Society of America Bulletin, v. 67, p. 1441–1474, doi:10.1130/0016-7606(1956)67[1441:SOTOLI]2.0.CO;2.
- Piotrowski, R. G., and J. A. Harper, 1979, Black shale and sandstone facies of the Devonian “Catskill” clastic wedge in the subsurface of western Pennsylvania: U.S. Department of Energy Eastern Gas Shales Project, Series 13, 40 p.
- Posamentier, H. W., and P. R. Vail, 1988, Eustatic controls on clastic deposition: II. Sequence and systems tract models, in H. W. Posamentier, C. K. Wilgus, B. S. Hastings, C. G. S. C. Kendall, C. A. Ross, and J. C. Van Wagoner, eds., Sea level changes—An integrated approach: SEPM Special Publication 42, p. 125–154.
- Prave, A. R., W. L. Duke, and W. Slattery, 1996, A depositional model for storm- and tide-influenced prograding siliciclastic shorelines from the Middle Devonian of the central Appalachian foreland basin, U.S.A.: *Sedimentology*, v. 43, p. 611–629, doi:10.1111/j.1365-3091.1996.tb02017.x.
- Rickard, L. V., 1984, Correlation of the subsurface Lower and Middle Devonian of the Lake Erie region: Geological Society of America Bulletin, v. 95, p. 814–828, doi:10.1130/0016-7606(1984)95<814:COTSLA>2.0.CO;2.
- Rickard, L. V., 1989, Stratification of the subsurface low and mid-Devonian of New York, Pennsylvania, Ohio, and Ontario: New York State Museum and Science Map and Chart Series 39, 59 p.
- Sageman, B. B., A. E. Murphy, and J. P. Werne, C. A. ver Straeten, D. J. Hollander, and T. W. Lyons, 2003, A tale of shales; the relative roles of production, decomposition, and dilution in the accumulation of organic-rich strata, Middle—Upper Devonian, Appalachian Basin; Isotopic records of microbially mediated processes: *Chemical Geology*, v. 195, p. 229–273, doi:10.1016/S0009-2541(02)00397-2.
- Scotese, C. R., and W. S. McKerrow, 1990, Revised world map and introduction, in W. S. McKerrow and C. R. Scotese, eds., Paleozoic paleogeography and biogeography, Geological Society (London) Memoir 12, p. 1–21.
- Shier, D. E., 2004, Well log normalization: Methods and guidelines: *Petrophysics*, v. 45, 268 p.
- Singh, P., 2008, Lithofacies and sequence stratigraphic framework of the Barnett Shale, northeast Texas: Ph.D. dissertation, University of Oklahoma, Norman, Oklahoma, 181 p.
- Slatt, R. M., and Y. Abousleiman, 2011, Merging sequence stratigraphy and geomechanics for unconventional gas shales: The Leading Edge, v. 30, p. 274–282, doi:10.1190/1.3567258.
- Slingerland, R., N. W. Driscoll, J. D. Milliman, S. R. Miller, and E. A. Johnstone, 2008a, Anatomy and growth of a Holocene clinothem in the Gulf of Papua: *Journal of Geophysical Research*, v. 113, p. F01S13, doi:10.1029/2006JF000628.
- Slingerland, R., R. W. Selover, A. S. Ogston, T. R. Keen, N. W. Driscoll, and J. D. Milliman, 2008b, Building the Holocene clinothem in the Gulf of Papua: An ocean circulation study: *Journal of Geophysical Research*, v. 113, p. F01S14, doi:10.1029/2006JF000680.
- Sloss, L. L., 1963, Sequences in the cratonic interior of North America: Geological Society of America Bulletin, v. 74, p. 93–114, doi:10.1130/0016-7606(1963)74[93:SITCIO]2.0.CO;2.
- Svendsen, J. B., and N. R. Hartley, 2001, Comparison between outcrop-spectral gamma ray logging and whole rock geochemistry: Implications for quantitative reservoir characterisation in continental sequence: *Marine and Petroleum Geology*, v. 18, p. 657–670, doi:10.1016/S0264-8172(01)00022-8.
- Tribouillard, N., T. J. Algeo, T. Lyons, and A. Riboulleau, 2006, Trace metals as paleoredox and paleoproductivity proxies: An update: *Chemical Geology*, v. 232, p. 12–32, doi:10.1016/j.chemgeo.2006.02.012.
- Van Wagoner, J. C., R. M. Mitchum, K. M. Campion, and V. D. Rahmanian, 1990, Siliciclastic sequence stratigraphy in well logs, cores, and outcrops: Concepts for high-resolution correlation of time and facies: AAPG Methods in Exploration 7: AAPG Special Volumes, Methods in Exploration, 55 p.
- ver Straeten, C. A., 1995, Stratigraphic synthesis and tectonic and sequence stratigraphic framework, upper Lower and Middle Devonian, northern and central Appalachian Basin: Rochester, New York, University of Rochester, 1600 p.
- ver Straeten, C. A., 1996, Upper Lower and lower Middle Devonian stratigraphic synthesis, central Appalachian Basin of Pennsylvania: Pennsylvania Geological Survey Open File Report, 4th Series, 59 p.
- ver Straeten, C. A., 2004, K-bentonites, volcanic ash preservation, and implications for Early to Middle Devonian volcanism in the Acadian orogen, eastern North America: Geological Society of America Bulletin, v. 116, p. 474–489, doi:10.1130/B25244.1.
- ver Straeten, C. A., 2007, Basinwide stratigraphic synthesis and sequence stratigraphy, upper Pragian, Emsian and Eifelian stages (Lower to Middle Devonian), Appalachian Basin, in R. T. Becker and W. T. Kirchgasser, eds., Devonian events and correlation: Geological Society (London) Special Publication 278, p. 39–81, doi:10.1144/SP278.3.
- ver Straeten, C. A., and C. E. Brett, 1995, Stratigraphy and facies relationships of the Eifelian Onondaga Limestone (Middle Devonian) in western and west central New York State, in C. E. Brett and J. Scatterday, eds., New York State Geological Association, 66th annual meeting guidebook: Field Guide, p. 221–269.
- ver Straeten, C. A., and C. E. Brett, 2000, Bulge migration and pinnacle reef development, Devonian Appalachian

- foreland basin: *Journal of Geology*, v. 108, p. 339–352, doi:[10.1086/314402](https://doi.org/10.1086/314402).
- ver Straeten, C. A., and C. E. Brett, 2006, Pragian to Eifelian strata (middle Lower to lower Middle Devonian), northern Appalachian Basin; stratigraphic nomenclatural changes: *Northeastern Geology and Environmental Sciences*, v. 28, p. 80–95.
- ver Straeten, C. A., C. E. Brett, and B. B. Sageman, 2010, Mudrock sequence stratigraphy: A multi-proxy (sedimentological, paleobiological, geochemical) approach, Devonian Appalachian Basin: *Palaeogeography, Palaeoclimatology, Palaeoecology*, v. 304, no. 1–2, p. 54–73, doi:[10.1016/j.palaeo.2010.10.010](https://doi.org/10.1016/j.palaeo.2010.10.010).
- West, M., 1978, Preliminary stratigraphic cross section showing radioactive zones in the Devonian black shales in the eastern part of the Appalachian Basin: U.S. Geological Survey Oil and Gas Investigations Chart OC-86.
- Wilkin, R. T., and M. A. Arthur, 2001, Variations in pyrite texture, sulfur isotope composition, and iron systematics in the Black Sea: Evidence for late Pleistocene to Holocene excursions of the O₂-H₂S redox transition: *Geochimica et Cosmochimica Acta*, v. 65, p. 1399–1416, doi:[10.1016/S0016-7037\(01\)00552-X](https://doi.org/10.1016/S0016-7037(01)00552-X).
- Wolosz, T. H., 1992, Patterns of reef growth in the Middle Devonian Edgecliff Member of the Onondaga Formation of New York and Ontario, Canada, and their ecological significance: *Journal of Paleontology*, v. 66, p. 8–15.
- Xie, X., and P. L. Heller, 2009, Plate tectonics and basin subsidence history: *Geological Society of America Bulletin*, v. 121, p. 55–64.